Structural Geology of the Bear River Formation (Halifax Group) and White Rock Formation (Rockville Notch Group) Contact in the Cape St. Marys area, southwest Nova Scotia

Carla Dickson

Submitted in Partial Fulfillment of the Requirement for the
Degree of Honours Bachelor of Science,
Department of Earth Sciences

At

Dalhousie University
Halifax, Nova Scotia
April, 2013

Submitted to: Dr. Nicholas Culshaw

Dr. Martin Gibling

Distribution License

DalSpace requires agreement to this non-exclusive distribution license before your item can appear on DalSpace.

NON-EXCLUSIVE DISTRIBUTION LICENSE

You (the author(s) or copyright owner) grant to Dalhousie University the non-exclusive right to reproduce and distribute your submission worldwide in any medium.

You agree that Dalhousie University may, without changing the content, reformat the submission for the purpose of preservation.

You also agree that Dalhousie University may keep more than one copy of this submission for purposes of security, back-up and preservation.

You agree that the submission is your original work, and that you have the right to grant the rights contained in this license. You also agree that your submission does not, to the best of your knowledge, infringe upon anyone's copyright.

If the submission contains material for which you do not hold copyright, you agree that you have obtained the unrestricted permission of the copyright owner to grant Dalhousie University the rights required by this license, and that such third-party owned material is clearly identified and acknowledged within the text or content of the submission.

If the submission is based upon work that has been sponsored or supported by an agency or organization other than Dalhousie University, you assert that you have fulfilled any right of review or other obligations required by such contract or agreement.

Dalhousie University will clearly identify your name(s) as the author(s) or owner(s) of the submission, and will not make any alteration to the content of the files that you have submitted.

If you have questions regarding this license please contact the repository manager at dalspace@dal.ca.

Grant the distribution license by signing and dating below.

_____ _____

Name of signatory Date

DALHOUSIE UNIVERSITY
Inspiring Minds

Department of Earth Sciences
Halifax, Nova Scotia
Canada B3H 4R2
(902) 494-2358
FAX (902) 494-6889

DATE: APRIL 25, 2013

AUTHOR: CARLA HELEEN DICKSON

TITLE: STRUCTURAL GEOLOGY OF THE BEAR RIVER FORMATION (HALIFAX GROUP) AND WHITE ROCK FORMATION (ROCKVILLE NOTCH GROUP) CONTACT IN THE CAPE ST. MARYS AREA, SOUTHWEST NOVA SCOTIA

Degree: B.Sc Convocation: May Year: 2013

Permission is herewith granted to Dalhousie University to circulate and to have copied for non-commercial purposes, at its discretion, the above title upon the request of individuals or institutions.

Signature of Author

Abstract

The contact between the Bear River Formation (BRF) (Halifax Group) and White Rock Formation (WRF) (Rockville Notch Group) at Cape St. Marys (CSM) is deformed at greenschist facies, but the exact nature of the contact is disputed. At the CSM "unconformity" cleavage in the BRF and WRF are parallel; and bedding in the WRF is parallel to the steeply SE-dipping contact and cleavage. Bedding in the BRF slate is more steeply dipping than the contact and displays asymmetric folds with the orientation of thickened short limb and thinned long limb, consistent with topside-up shear (SE, WRF side). The deformed folds are accompanied by intense cleavage with down-dip stretching lineation (quartz fringes on pyrite). With increased distance across strike NW from the contact the zone of intense cleavage is replaced by a narrow interval of open folding bound by another zone of intense cleavage. In all zones of BRF, intersection of bedding and cleavage has subhorizontal to moderately steep plunge, suggesting heterogeneous deformation and the close angle between S_0/S_{x1} fabric and the S_{x2} fabric imply the rocks have experienced a high strain. No crenulation fabric was observed in the study area, however crenulations have been observed further southeast within the Cape St. Marys Shear Zone. No evidence of a discrete fault was observed at or near to the contact, therefore deformation was continuous across the contact and the units were deformed in-situ.

Vertical *Arenicolites* paired burrows in the intensely cleaved BRF slate function as paleo-plumblines with respect to bedding. Burrows are now boudined down-dip parallel to the quartz fringe lineation and lie within the S_{x2} cleavage; the WRF dacite contains down-dip stretched lapilli also within the S_{x2} cleavage, therefore there has been extension in the down-dip direction of the S_{x2} cleavage plane. The burrows lie approximately 10° to bedding indicating a high degree of shear strain associated with the transposed bedding. The BRF slate also contains rigid pyrite crystals that disturbed the stress field and flow pattern around them during deformation. Sides of the pyrites normal to the minimum compression are low strain areas within which quartz strain fringes formed in the direction of the instantaneous stretching axis (ISA). The strain fringes are important not only because they produced the macroscopic down-dip lineation but also recorded part of the progressive deformation history of the host-rock and indicate the degree of non-coaxiality of deformation and the finite strain.

The interpretations of this thesis lead to the overall conclusion that the Bear River Formation and the White Rock Formation deformed in-situ and did so by White Rock Formation side-up plane strain simple shear across the region, where the direction of shear has been interpreted from sheared folds.

Table of Contents

List of Figures

List of Tables

Terminology

Stress: (differential) magnitude of force applied to an area is greater in one direction

Tensional/Extension Stress: force that tends to stretch and thin or fault rock

Strain: a rocks response to stress; deformation resulting in change of shape or position

Plastic Deformation: deformation is permanent, rock flows in response to stress, and materials will not return to original shape after stress is removed

Brittle Deformation: deformation is permanent, rock fractures in response to stress, and materials will not return to original shape after stress is removed

Transposition: the overprinting of an older cleavage foliation by a younger foliation due to stronger deformation, and can be considered evidence for multiple deformation events (for the purpose of this project)

Shear Angle: the angle between pairs of lines that were initially perpendicular

Plane Strain: (plane deformation) is a special state of strain where the strain of a three-dimensional body for which there is not deformation parallel to the intermediate principal axis. Due to this condition, plane strain can be analyzed as a two-dimensional strain.

2D Pure Shear: is a constant-volume plane strain. Material lines parallel to the principal strain axes do not rotate and do not undergo shear strain. Material lines of other orientations in the strain plane rotate toward s_1.

Simple Shear: is a constant-volume plane strain where the displacement of all material particles is parallel to the shear plane. In the strain plane all material lines except those parallel to the shear plane are rotated.

Progressive Deformation: non-rigid motion of a body which carries the body from the initial undeformed state to the final deformed state. Strain states the body passes through during the progressive deformation define the strain path.

Abbreviations

pyr: pyrite

qtz: quartz

cal/dol: calcite or dolomite (specific carbonate type unknown)

act: actinolite

chl: chlorite

psc: pressure solution cleavage

ml: microlithons

BRF: Bear River Formation

HG: Halifax Group

WRF: White Rock Formation

XPL: cross-polarized light

PPL: plane-polarized light

Acknowledgements

I would like to extend my sincerest gratitude to my supervisor, Dr. Nicholas Culshaw for providing me with the opportunity to work on a project that was both challenging and interesting, for shepherding me through the writing process, and for showing patience with my endless questions. It was a pleasure to work with someone who is so fascinated by the world, determined to figure out how all the pieces work. I would also like to thank Dr. Martin Gibling for his guidance through the writing process, for his advice on presentations, and for his persistence in helping the students do well. Thank you to Dr. Grant Wach and everyone in the Basin & Reservoir Lab for helping and tolerating me for the past year while I worked on my thesis. I would like to thank the entire faculty and staff of the Dalhousie University Earth Science department and my classmates for their tremendous support, instruction, and advice during my undergraduate degree and this thesis.

Finally, I must give my deepest thanks to my family for their continued support throughout my education, particularly during the completion of this thesis; you pushed me when I struggled and listened when I needed to sounding board.

Chapter I: Introduction

1.1 Statement of Problem

The contact between the Bear River Formation (Halifax Group) and White Rock Formation (Rockville Notch Group) at Cape St. Marys is deformed at greenschist facies, but the exact nature of the contact is disputed: did the units deform together in-situ or was there relative displacement as they deformed?

The objective of this study is to better define the structural conditions and origin of the deformed contact between the Bear River and White Rock formations at Cape St. Marys. Structures in this area have been incompletely studied, and detailed information on strain and kinematics is needed to better understand the deformation of the rocks. It is important to complete this study as the Cape St. Marys area occupies a significant position in the Appalachian Orogen, in a zone of Alleghanian overprinting of Neoacadian structures (Culshaw & Liesa, 1997).

The objective of this project was achieved by collecting oriented samples and measurements in the study area to complete a structural analysis and mapping of the deformed contact. The structural analysis included a kinematic analysis to determine if thrust or extensional shear was responsible for observed structures. The kinematic analysis included a study of the meso-structures and micro-structures, and the relationships between them, as kinematic indicators of deformation.

1.2 Geological Setting & Tectonic Evolution of Cape St. Marys

The multifaceted tectonic evolution of the Appalachian Orogen is the reason for the complex structures observed in outcrop and map. The accretion and subsequent deformation of multiple terranes with the Laurentian continent formed the Appalachian Orogen during the building of Pangea and concluded with the collision of Laurentia and Gondwana (Murphy & Nance, 2008). The Appalachian Orogen was a result of three phases of mountain building: the Taconic phase, the Neoacadian phase, and the Alleghanian phase (Figure 1.1).

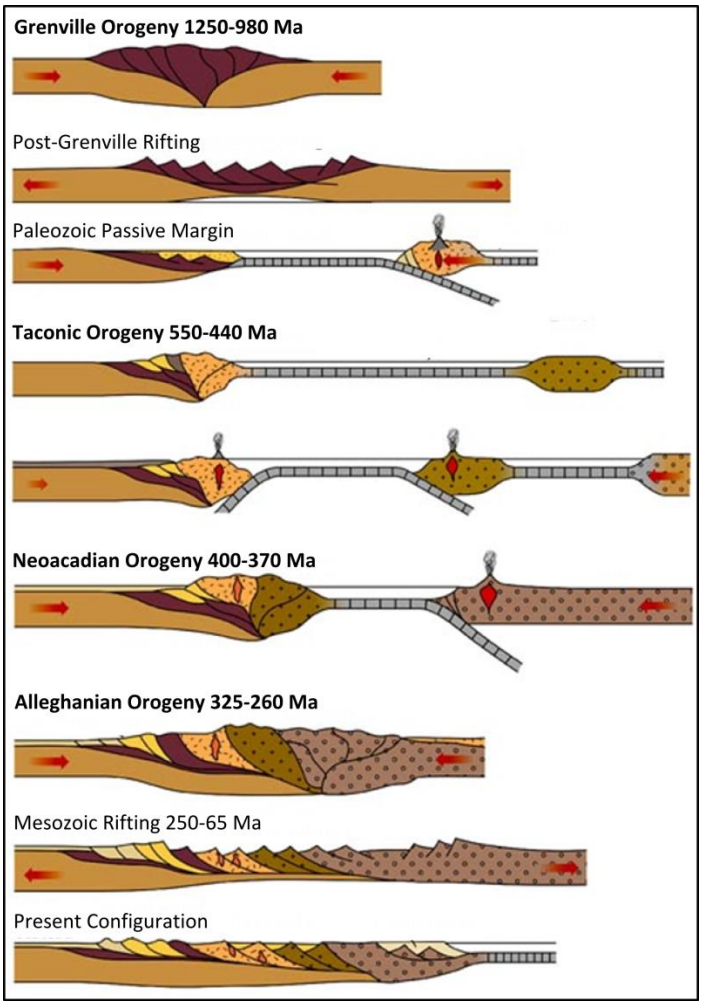

Figure 1.1: Tectonic formation of present-day east coast North American plate from Mesoproterozoic to Present (Marshak, 2012).

Cape St. Marys is located in the Meguma Terrane of Nova Scotia, which is comprises the Gander, Avalonia, and Meguma terranes (Figure 1.2) The Meguma Terrane is normally considered to have originated as a peri-Gondwanan terrane (precise position along the margin of Gondwana is unknown), where the material forming the Halifax and Goldenville groups was deposited on a continental rise or outer shelf slope of a passive margin near to Laurentia (White & Barr, 2012). The Meguma Terrane is also interpreted to have been part of and travelled with Avalonia (Murphy & Nance, 2008). Either theory regarding the Meguma Terrane times the deposition of the material forming the terrane during the Cambrian (541-485 Ma); therefore they were deposited synchronously with the Taconic phase of the Appalachian Orogeny and are not believed to have deformed (or recorded evidence of) during this phase. Instead, the rocks deformed during the progressive collision of Laurentia and Gondwana (with microcontinents between).

The second phase of the Appalachian Orogeny, the Neoacadian phase, occurred during the Devonian (400-370 Ma) and was the first to affect the Meguma Terrane rocks (would eventually be deposited at Cape St. Marys). The Avalonia island arc converged obliquely from the northeast to the Laurentia landmass (Keppie & Dallmeyer, 1987). The collision created and reactivated regional faults, and caused rocks, to be metamorphosed and deformed. The Neoacadian phase caused the formation of large northeast-trending upright folds with steep axial planar cleavage (F_1), and was the first significant deformation event (D_1) (Keppie & Dallmeyer, 1987). The convergence of the plates during the Taconic phase and the Neoacadian phase were the early stages of the formation of Pangea (Murphy & Nance, 2008).

The third phase of the Appalachian Orogeny, the Alleghanian phase, occurred during the Late Carboniferous to Permian (325-260 Ma) and was the second to affect the Cape St. Marys area. Gondwana completed the collision with Laurentia and the supercontinent Pangea formed. As the continents collided rock material trapped between them was uplifted and frequently pushed far inland (Murphy & Nance, 2008). Large belts of material bordered by thrust sheets stacked on top of each other, shortening the eastern margin on Laurentia (southeast United States to Newfoundland). The collision also formed folds that were perpendicular to the collision (forces northwest-southeast, fold trends northeast-southwest). In Nova Scotia, this formed inclined, northwest-vergent reworked Neoacadian fold domains (F_2) with adjoining shear zones, and was the second major deformation event (D_2) affecting the rocks of interest (Keppie & Dallmeyer, 1995). The Meguma Terrane remained attached to Laurentia during the rifting of Pangea in the Early-Middle Jurassic, becoming the southern half of Nova Scotia (Keppie & Dallmeyer, 1987; Murphy & Nance, 2008).

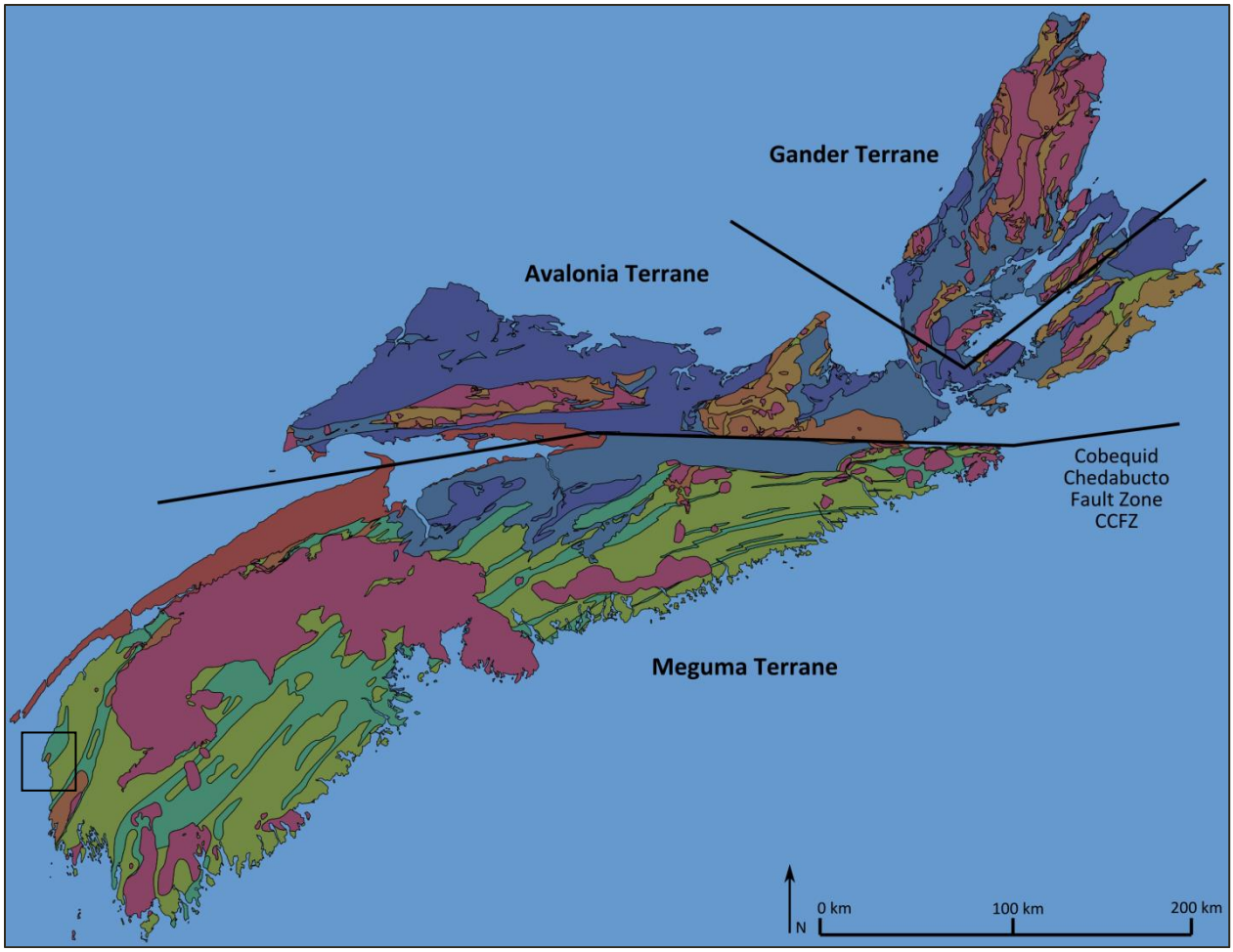

Figure 1.2: Bedrock geology map of Nova Scotia showing location of Cobequid-Chedabucto Fault Zone separating the Avalonia terrane and Gander terrane from the Meguma Terrane. Study area is located within black box in southwest corner of map (modified from Keppie, Fisher, & Poole, 2006).

1.3 Study Area

The study area is located 35 km north-northwest of Yarmouth, and is a coastal section on the Gulf of Maine (Figure 1.3). The area has simple map-scale geology with good coastal exposures, making field work straightforward. This area has been studied by several geologists as it appeared interesting when observed; the curious puzzle of the deformed “unconformity”, which has experienced Neoacadian then Alleghanian deformation, was examined and required an explanation (Figure 1.4).

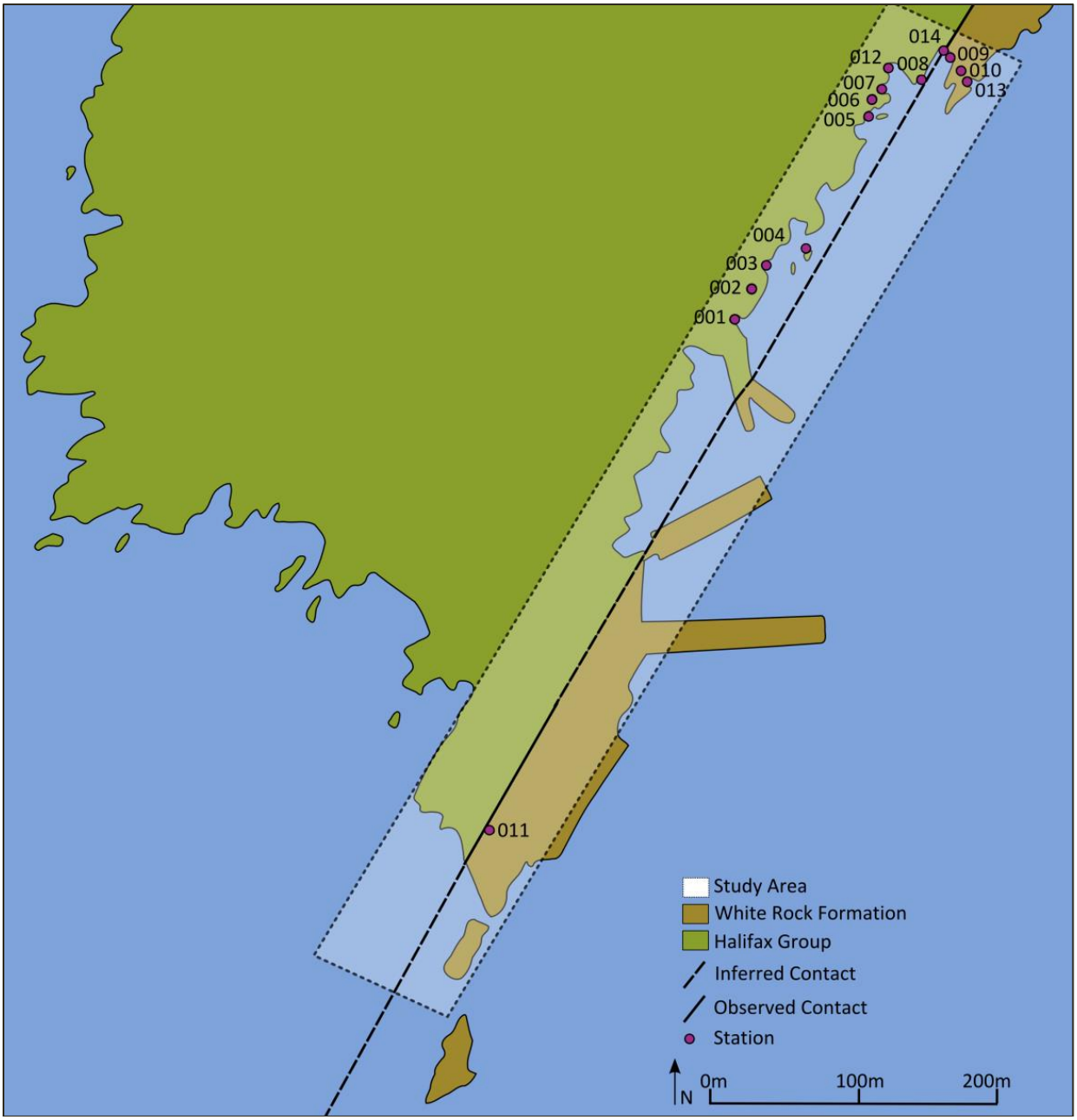

Figure 1.3: Bedrock geology map of Cape St. Marys and surrounding area, southwest Nova Scotia with study area outlined and station locations indicated.

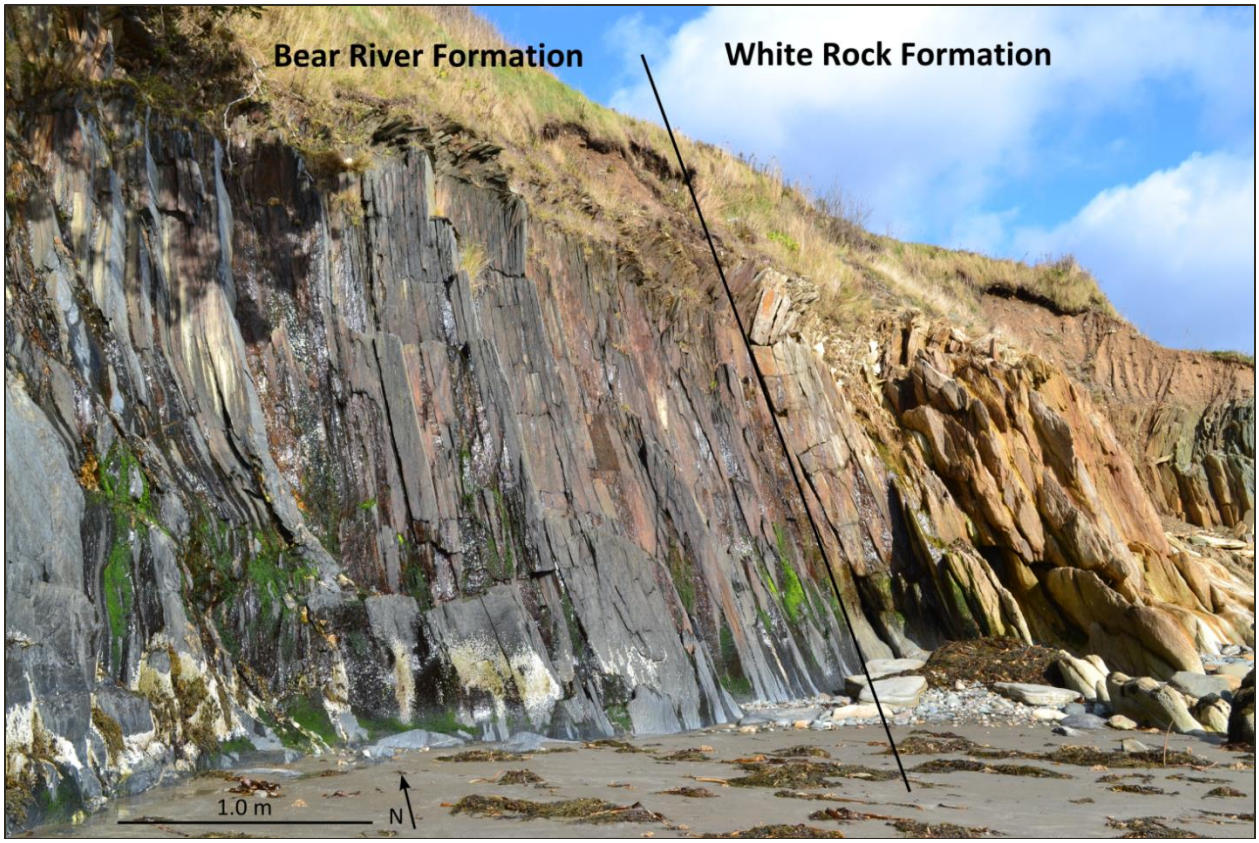

Figure 1.4: Coastal outcrop of contact between Bear River Formation and White Rock Formation at Cape St. Marys study area (Station 014).

1.4 Previous Work

The geology at Cape St. Marys and surrounding region has been extensively studied in order to better understand the age, structure, metamorphism, and stratigraphy. Time constraints on Late Paleozoic collision, delamination, magmatism, age of shear zones, and age of detrital and metamorphic rocks have all been examined using $^{40}Ar/^{39}Ar$ dating methods (Keppie & Dallmeyer, 1995; Culshaw & Reynolds, 1997; Hicks, Jamieson, & Reynolds, 1999). The stratigraphy, metamorphism, paleontology, and provenance of the Meguma terrane have been investigated by many geologists, especially the relationship between the Goldenville and Halifax groups (White, 2010; White & Barr, 2012).

The previous research of particular interest for this project focused on tectonic and structural focused, including studies by Culshaw and Liesa (1997) on the Alleghanian reactivation of the (Neo) Acadian fold belt in southwest Nova Scotia, and by Culshaw and Lee (2006) on the geometry and genesis of the fold belt and constraints on the tectonics of the Meguma terrane. Culshaw and Liesa (1997) concluded shear zones and folds delineate a belt of deformation that overprinted the (earlier-formed) Acadian fold belt; the shear zones formed a system that permitted convergence-dominated transpression of the Meguma on an erratic Avalon border; the age for the overprinting is Alleghanian, with reactivation of Meguma basement structures; and the structures can be used to define a belt of Alleghanian deformation across the northwest Meguma Terrane. Culshaw and Lee (2006) concluded there are two orders of folding in the Meguma Terrane; the geometry of the main phase of folding was influenced by detachment forming a soft, thick shear zone; granite production may have been initiated by mantle delamination during the formation of Pangea; and later deformation occurred as a result of displacement of the Meguma Terrane along the CCFZ.

Evidence for Silurian continental rifting from the petrology, age, and tectonic setting of the White Rock Formation has been studied in the region by MacDonald et al. (2002). They dated a felsic tuff from the upper White Rock Formation using U-Pb zircon methods to get Silurian age of 438 Ma, which is consistent with previously determined ages for the Brenton Pluton and volcanic rocks at the base of the White Rock Formation. They also studied the geochemical characteristics and concluded an alkali affinity and a continental within-plate setting, and suggested the igneous activity may have occurred as a result of extension of the Meguma when it rifted off Gondwana.

Chapter 2: Regional Geology

Regional geology of the Meguma terrane in Nova Scotia is well understood from mapping and petrological studies that have constrained the stratigraphy into well-defined units. For this study, the Meguma Supergroup and the Rockville Notch Group of the Meguma terrane will be emphasized, separated by an unconformity that spanning approximately 23 million years. The type of unconformity (disconformity, angular unconformity, etc.) cannot be determined due to the degree of deformation.

2.1 Meguma Supergroup

In southwestern Nova Scotia, the Meguma Supergroup is subdivided into the Goldenville Group and the Halifax Group (Figure 2.1). The Goldenville Group is the basal unit (overlain by the Halifax Group), and is assumed to be in contact with the basement.

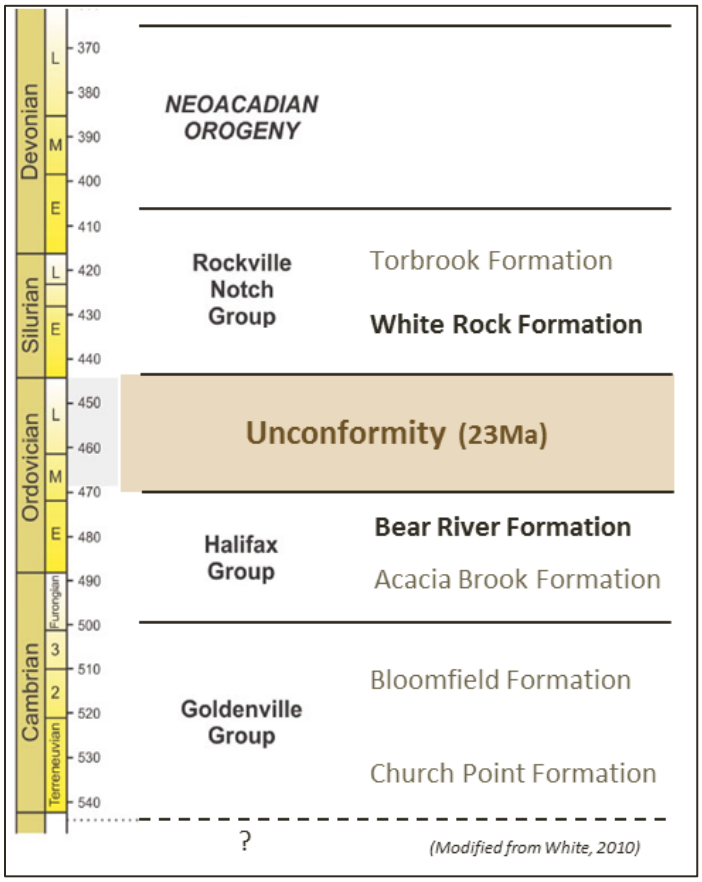

Figure 2.1: Stratigraphic chart of southwestern Nova Scotia near Chebogue Point Shear Zone. Note the unconformity between 445 and 468 Ma, which is represented by the contact of the Halifax Group and the Rockville Notch Group at Cape St. Marys (modified from White & Barr, 2012).

2.1.1 Goldenville Group

The Cambrian-Ordovician Goldenville Group is predominantly metasandstones, and is subdivided into six formations (in Nova Scotia): Bloomfield Formation, Church Point Formation, Moshers Island Formation, Government Point Formation, Green Harbour Formation, and Moses Lake Formation (White, 2010). The Bloomfield Formation occurs northeast of Cape St. Marys, and is a metasiltstone dominated unit at the top of the Goldenville Group (Figure 2.1). The formation comprises thin- to medium-thick beds of purple and grey metasilstones and slates that are rarely interbedded with thin, fine grained, poorly sorted metasandstone layers (White, 2010). The lithology of the formation suggests that it may have been deposited in a turbidity current environment. It varies in thickness from 200-400 m in the southwest limb, up to 1000 m in the northwest; this variation is explained by transposition and thickening of the Chebogue Point and Cape St. Marys shear zones (White, et al., 2001). The Goldenville Group will not be discussed further in this thesis, however as it is the other unit in contact with the Halifax Group a brief description has been included.

2.1.2 Halifax Group

The Goldenville Group is conformably overlain by the Halifax Group, which can be subdivided into four formations: Bear River, Acacia Brook, Feltzen, and Cunard formations. The Bear River and Acacia formations are visible on the limbs of the Cape St. Marys syncline (White, 2010). The Acacia Formation is the base unit of the Halifax Group in the region, and is 820 m section of predominantly slate interlayered with thin beds of metasiltstone and metasandstone. There are sulphide minerals and graphite, which suggests deposition in an anaerobic marine environment (Waldron, 1992).

The Bear River Formation is the upper unit of the Halifax Group in southwestern Nova Scotia, and is well exposed at Cape St. Marys where it is in contact with the overlying White Rock Formation (exact nature of this contact is disputed, and is the focus of this paper) (White, 2010). The Bear River Formation is predominantly metasiltstone interbedded with thin layers of slate and fine-grained metasandstone layers. Sulphide minerals are present in less concentration than in the Acacia Formation (White, 2010). The formation is thought to have been deposited in an upper slope to muddy shelf environment (Schenk, 1997).

2.2 Rockville Notch Group

The Rockville Notch Group is restricted to the northwest of the Meguma terrane; the basal unit is the White Rock Formation, which forms the southeastern side of the contact at Cape St. Marys (northwestern side is the Bear River Formation of the Halifax Group). This is overlain by the Kentville Formation, which is overlain by the uppermost units – the New Canaan and Torbrook Formations (White, 2010). The Kentville, New Canaan and Torbrook formations are not discussed further, as they do not occur within the study area are beyond the scope of this project.

2.2.1 White Rock Formation

The Silurian to Early Devonian White Rock Formation is exposed within the Cape St. Marys syncline, and has a quartzofeldspathic base that is overlain by interbedded quartize and pelitic/semi-pelitic phyllite, with occasional thin basalts (Hwang, 1985). At Cape St. Marys pelites and semi-pelites are less common, forming approximately one-third of the section (low outcrops approaching the unconformity from Cape St. Marys beach) and the formation is

largely felsic volcaniclastics, quartzites, and basaltic dykes. The felsic volcaniclastics are geochemically consistent with within-plate genesis (MacDonald, et al., 2002).

2.3 Metamorphism and Deformation

The Meguma Supergroup and White Rock Formation were deformed and metamorphosed during the Neoacadian phase of the Appalachian Orogeny, under greenschist facies (Raeside & Jamieson, 1992; Culshaw & Reynolds, 1997; White, 2003). The metamorphism in the region is variable, with increased metamorphic grade to the south-southwest of Cape St. Marys, from chlorite zone (Meteghan to Cape St. Marys), to biotite zone (Cape St. Marys to Yarmouth), and garnet zone (Yarmouth syncline) (Figure 2.2) (Culshaw & Liesa, 1997). Several $^{40}Ar/^{39}Ar$ studies suggest that the greenschist facies metamorphism found in most of the Meguma terrane occurred approximately 400-377 Ma, during the early Neoacadian phase of the Appalachian Orogeny (Hicks et al. 1999; Keppie et al, 2002).

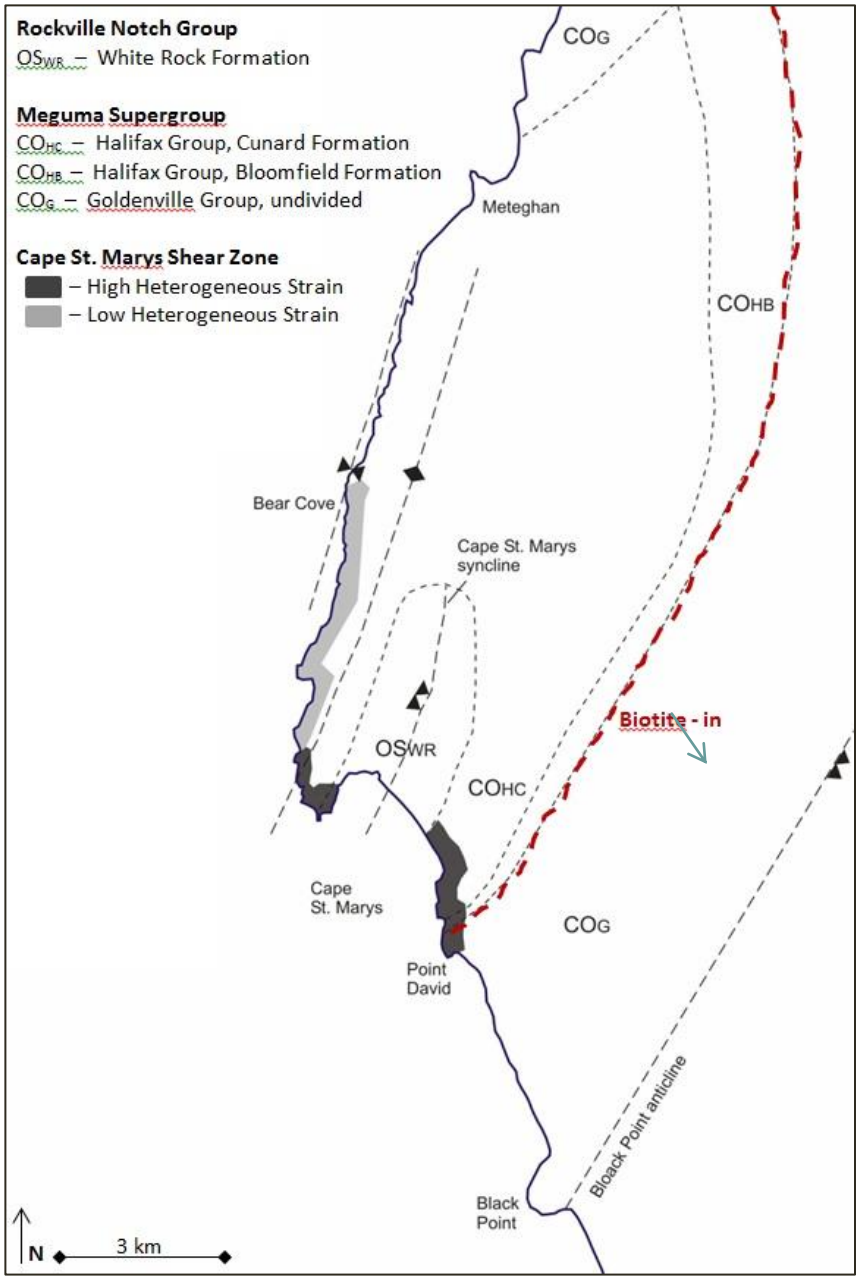

Figure 2.2: Simplified geological outline of Cape St. Marys region showing the Cape St. Marys shear zone, axial traces of the Bear Cove synclinorium, and the approximate regional metamorphic zone (isograd) of first appearance of index mineral (labelled) observed from shoreline only (more index minerals visible on larger map available in original from Culshaw & Liesa, 1997).

It is generally accepted the Meguma terrane was pervasively folded and metamorphosed during the Neoacadian phase (400-370 Ma), forming large, northeast-trending folds with steep axial planar cleavage (formation of these folds discussed in greater detail in Section 1.1: Geological Setting) (Keppie & Dallmeyer, 1987). There is increased evidence for reactivation and additional deformation of these early structures, and thermal overprinting

during the Alleghanian phase (325-260 Ma). Alleghanian overprinting on Neoacadian structures occurs within a wide zone of deformation (approximately 35 km map-view), resulting in southwest plunging reworked Neoacadian fold domains bounded by Carboniferous ductile shear zones (Keppie & Dallmeyer, 1995; Culshaw & Liesa, 1997). This is substantiated by studies on Neoacadian muscovite ages in southwest Nova Scotia, which were reset during the Carboniferous; later $^{40}Ar/^{39}Ar$ study of the syn-deformational muscovite grains in pyrite fringe structures indicated the age of the second phase of deformation as 320 ± 5Ma (Culshaw & Reynolds, 1997). These ages suggest partial to complete resetting of the argon during the Alleghanian phase representing shear-zone activity in the study area (relating closing temperature to metamorphic grade).

Chapter 3: Methods

3.1 Field Work

Measurements and samples were collected over several trips to the Cape St. Marys region in August, October and November of 2012, including bedding, lineation, and cleavage fabrics from 14 stations in the field area were measured and were then used to interpret the bedrock geology and structural characteristics. In 2005 multiple samples were collected, of which two were used in this study; nine additional oriented samples were collected during fieldwork in October and November 2012. Two samples were collected from the Bear River Formation slate, one as close to the contact as possible, and the other from further down the unit. In the White Rock Formation dacite two samples were collected – one as close to the contact as possible, and the other on the east boundary of the unit. One sample was collected from the greenschist basalt from approximately the middle of the outcrop. No sample was collected from the quartzite unit of the White Rock Formation as a sample had previously been collected (Foster, 2005). All sample orientations were measured in-situ before they were removed so any thin sections would be properly oriented with respect to the outcrop.

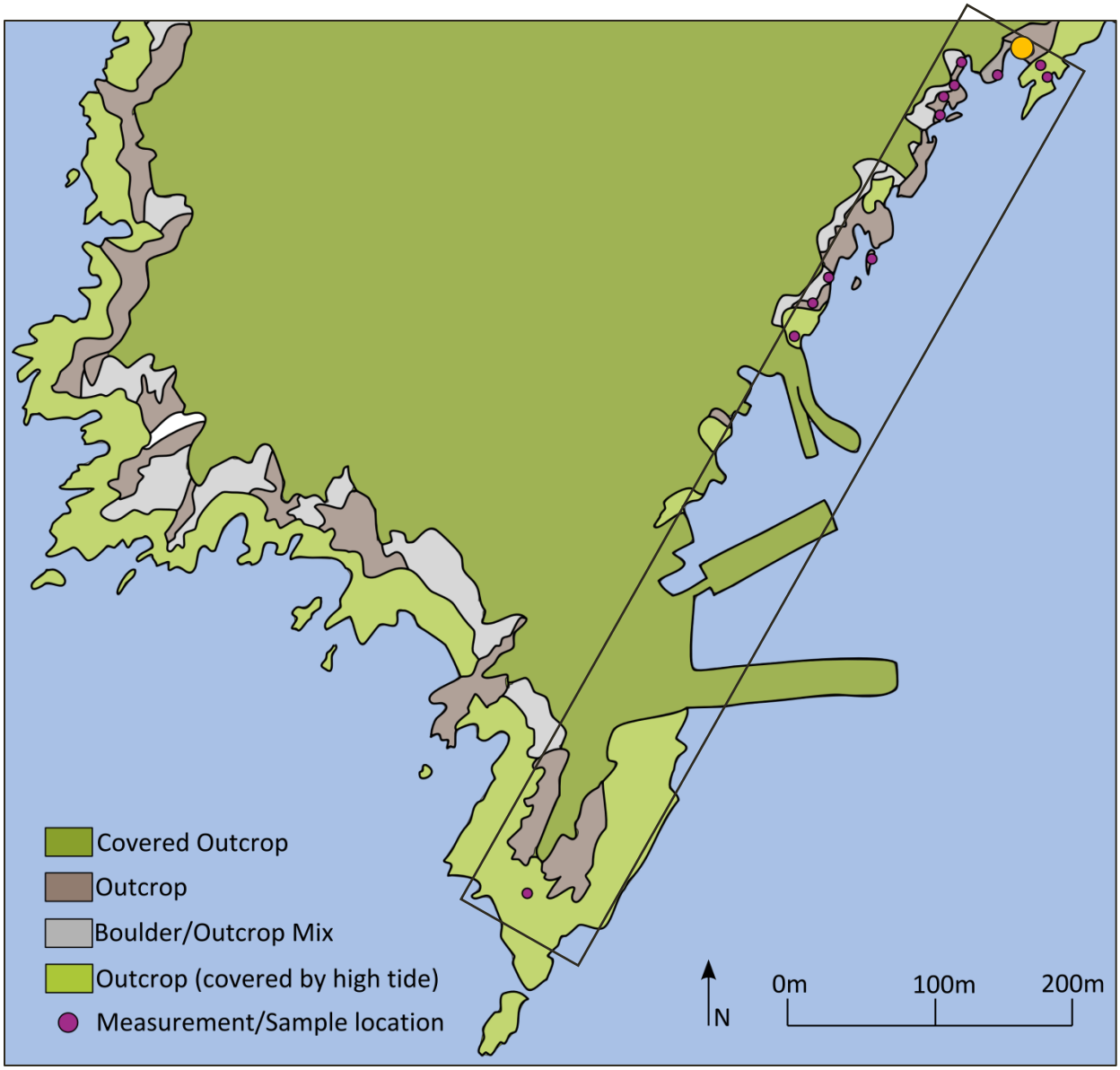

Figure 3.1: Map of field area (inside black box) including locations of measurements and samples (modified from Google Earth satellite image, 2005). The covered outcrop is obscured by soil, roads, buildings, etc. so the coastal outcrop provides the best opportunites for close examination. Location of Figure 3.2 shown in northwest corner (yellow circle).

A photo array of the outcrop was completed along with more focused photos of each unit (Figure 3.2). The contact and interesting features (preserved burrows, down-dip stretched lapilli, etc.) were also documented. High-quality documentation was critical in this thesis as the field site is fairly distant (approximately 300 km from Halifax, Nova Scotia), and access is tide

dependent (outcrop is only accessible within two to three hours of a low-tide). Weather was also an important consideration, as high waves and storms quickly changed the appearance of the outcrop between field trips, and entirely covered the most southwestern outcrop (Hurricane Sandy, October 22-31, 2012).

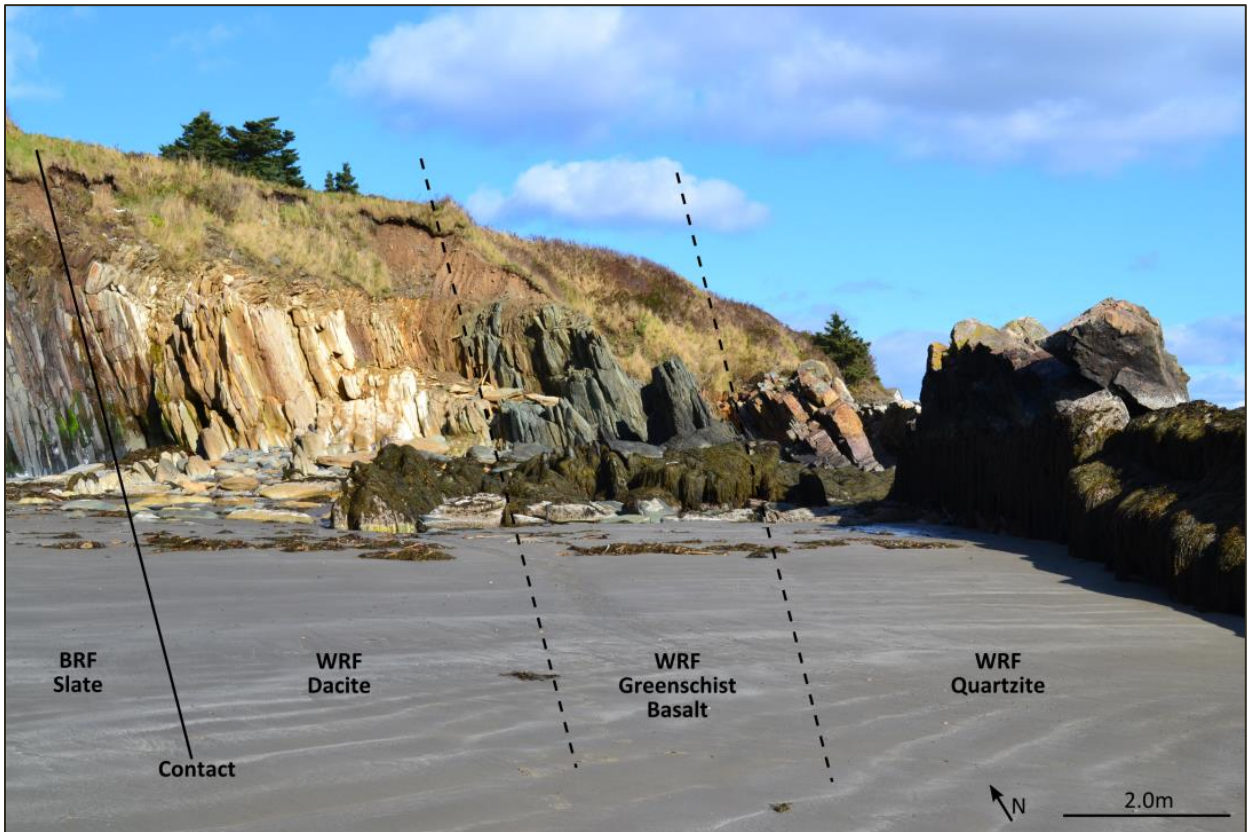

Figure 3.2: Outcrop photo showing location of WRF quartzite, greenschist basalt, and dacite relative to the contact with the BRF slate. Note this figure is only a partial section of the outcrop visible at Cape St. Marys, and that the WRF units appear conformable and parallel to the contact. Photo location shown on Figure 3.1.

3.2 Petrography

Field photos (2012 collection) were taken before samples were removed from outcrop. From the total eleven samples, 20 representative thin sections (18 normal and 2 polished) were prepared at the Dalhousie University thin section preparation lab. Petrography was completed

in the Dalhousie University microscope lab using a Nikon 50i transmitted-light microscope and images were captured using a Nikon Eclipse camera (50i Pol, LV-UEP1).

Petrographic and textural observations were recorded for each thin section, and a systematic process was required to keep the data organized (excel spreadsheet). This organization system was most important in the analysis of 219 pyrite core-objects and their associated strain-fringes from the Halifax Group slate for grain shape, location (group or isolated), dimension (equal or elongated), sense of shear (dextral, sinistral, or unknown), recrystallization of fringe, and fringe growth (face or displacement-controlled) (full results table available in Appendix I).

3.3 Strain Analysis

Rigid objects, such as pyrite crystals, can produce disturbances in the flow pattern of a deforming matrix, which can lead to the development of aggregates on the object known as strain fringes (Passchier & Trouw, 2005). The core-object and strain fringe together are known as fringe structures. The fringes are suspected to grow synchronous to deformation, therefore record (part) of deformation of the rock (Koehn, Bons, & Passchier, 2003). For this reason, they can be used as kinematic indicators for structural analysis to determine shear sense. The shape and orientation of the core-object (with respect to the instantaneous stretching axis) can lead to the development of different fringe shapes. The core-object and fringes can also rotate with respect to each other; however elongated core-objects and their strain fringes generally demonstrate less rotation (Figure 3.3).

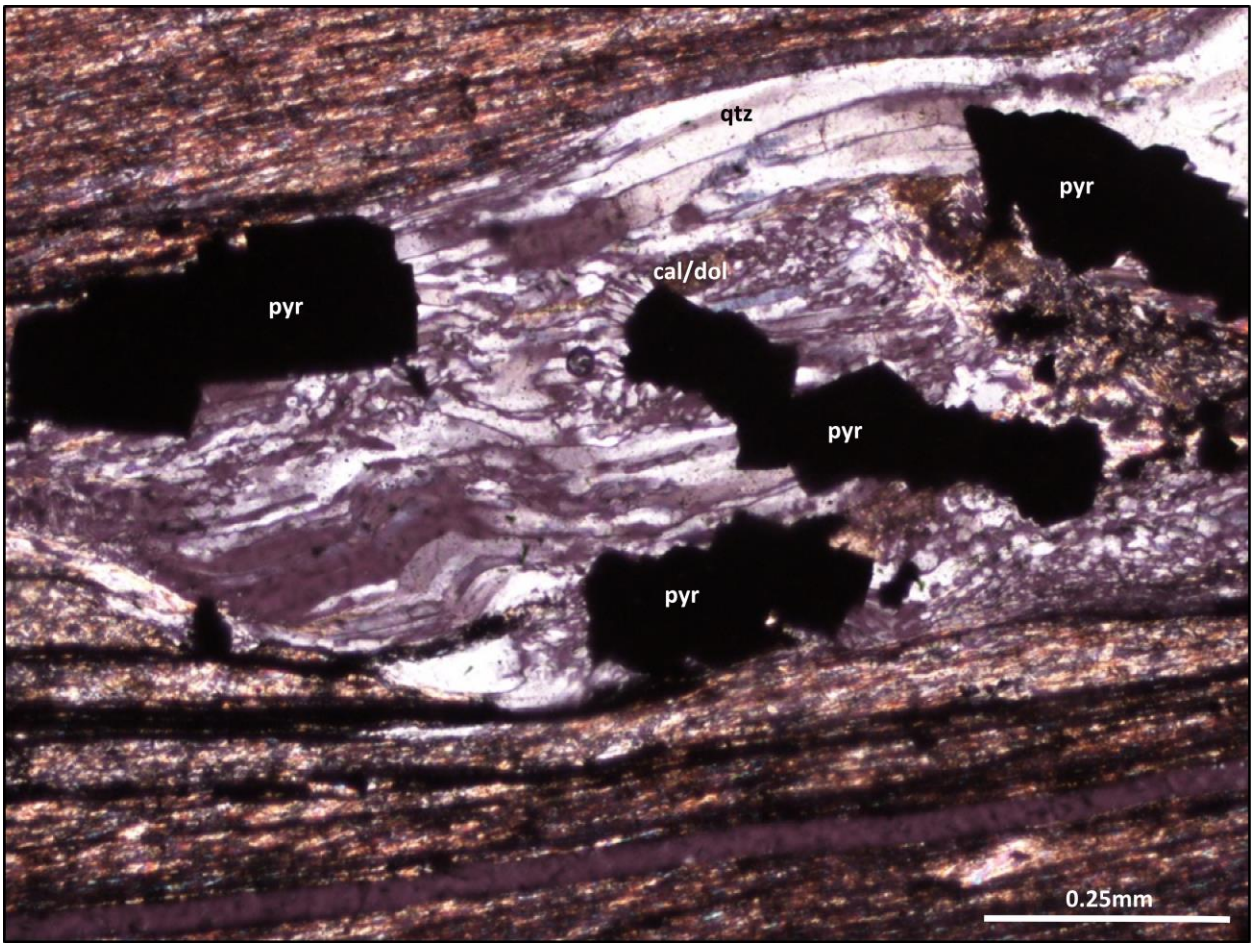

Figure 3.3: XPL thin section image showing elongated and more equidimensional pyrite core-objects and their associated quartz and carbonate strain fringes (together known as fringe structure) (Sample CD_12_001a, Station 014).

Strain analysis was completed on preserved burrows in the BRF slate. An oriented sample was measured and photographed before it was removed from the outcrop. The sample was then transferred to the Dalhousie University thin section preparation lab where the fissile, fragile sample was glued. The rock was cut perpendicular to strike through the centre of a burrow, which allowed the extension and rotation of the burrow relative to its original orientation to be quantified. The degree of extension was quantified by determining which grains lining the edge of the burrow represented original material (used by the organisms as

they burrowed) and which grains were a product of the extension (Figure 3.4 A&B). The original length of the burrow was calculated by summing the size of the grains established as original to the structure. This original length was subtracted from the current length, providing the change in length. The change in length of the burrow was divided by the original length of the burrow to give the degree of extension. The shear angle (rotation of the burrow relative to original position which is assumed to be perpendicular to bedding) was determined by measuring the angle of the burrow relative to the bedding, and from the shear angle the shear strain was calculated using the formula $\gamma \equiv \tan \Psi$ (assuming simple shear) (Twiss & Moores, 2006).

Figure 3.4A: Three paired Arenicolites burrows preserved in the BRF of the Halifax Group Slate (lens cap for scale, 3cm) (Station 004).

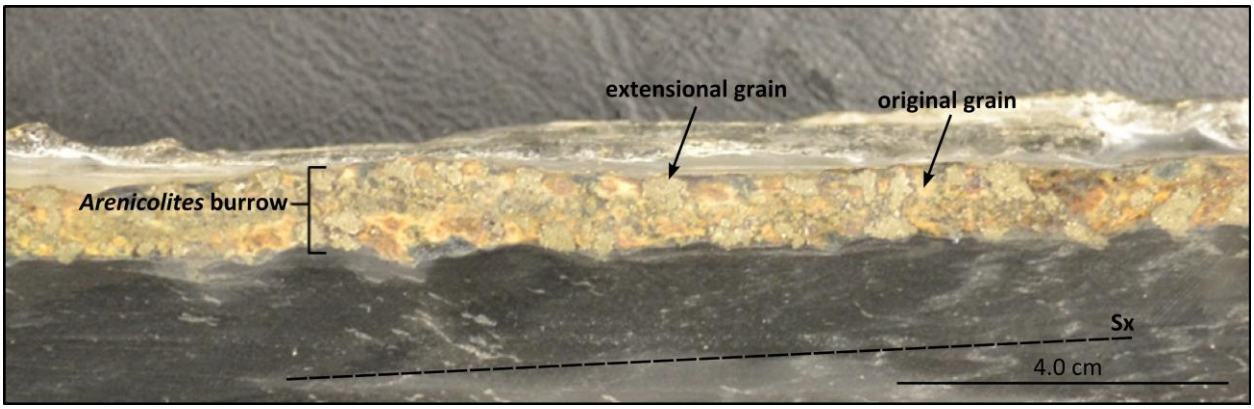

Figure 3.4B: Oriented cut sample of preserved Arenicolites burrow from BRF slate with original grains (orange-beige) and grains as a product of extension (beige) indicated.

The lineation measurements collected in both the HG and the WRF were plotted onto a stereonet to confirm whether they occurred in the same plane.

Chapter 4: Structural Geology Results

Measurements collected at the 14 stations were plotted onto a basemap of the Cape St. Marys area as separate maps for bedding, lineation, early-stage cleavage, and late stage cleavage (Figures 4.1 A-E).

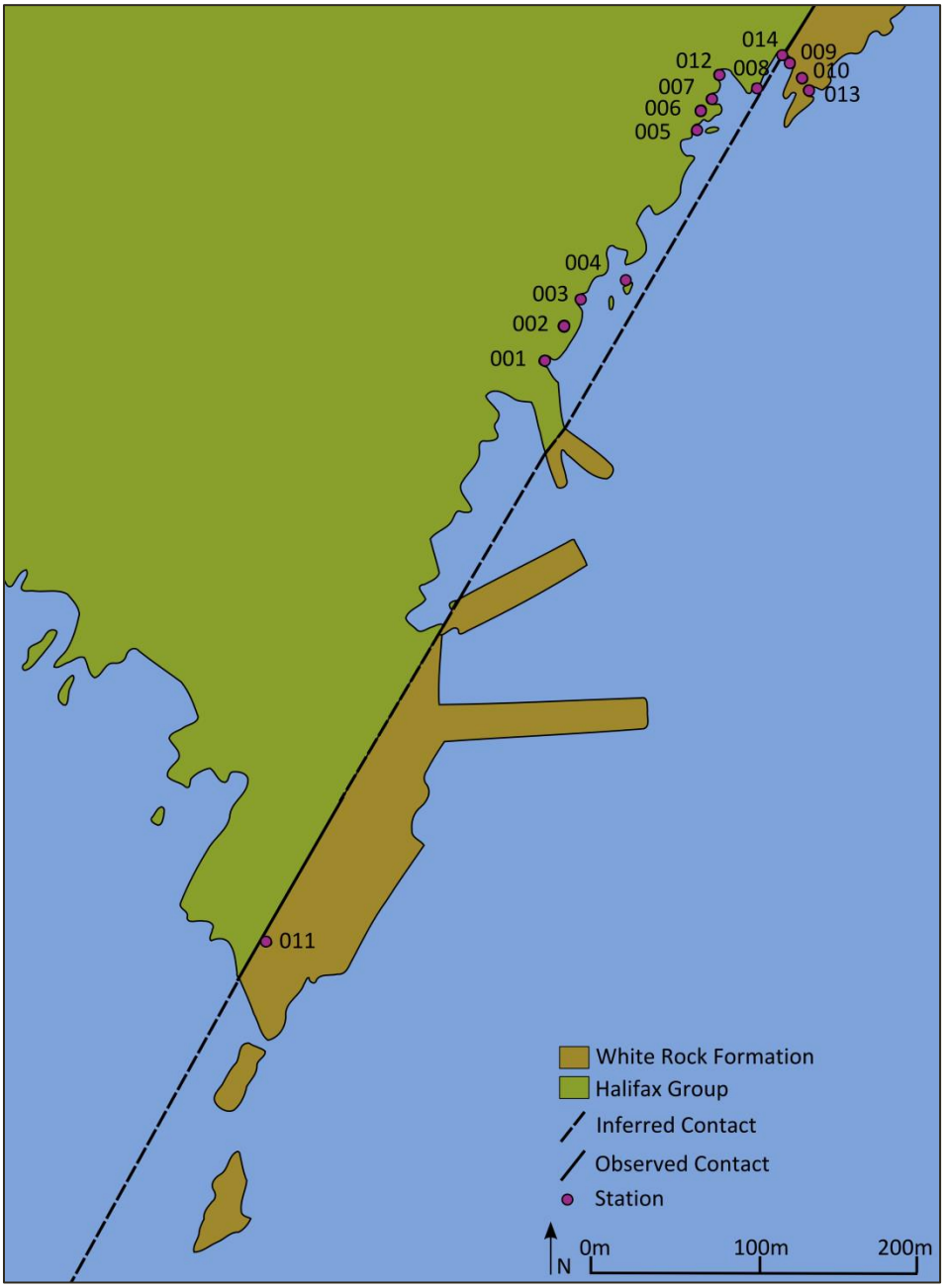

Figure 4.1A: Bedrock geology map of Cape St. Marys constructed from observations collected over the course of this thesis showing location of 14 stations.

Bedding measurements were recorded at nine stations, with strike generally trending northeast-southwest, moderately to steeply dipping (Figure 4.1B).

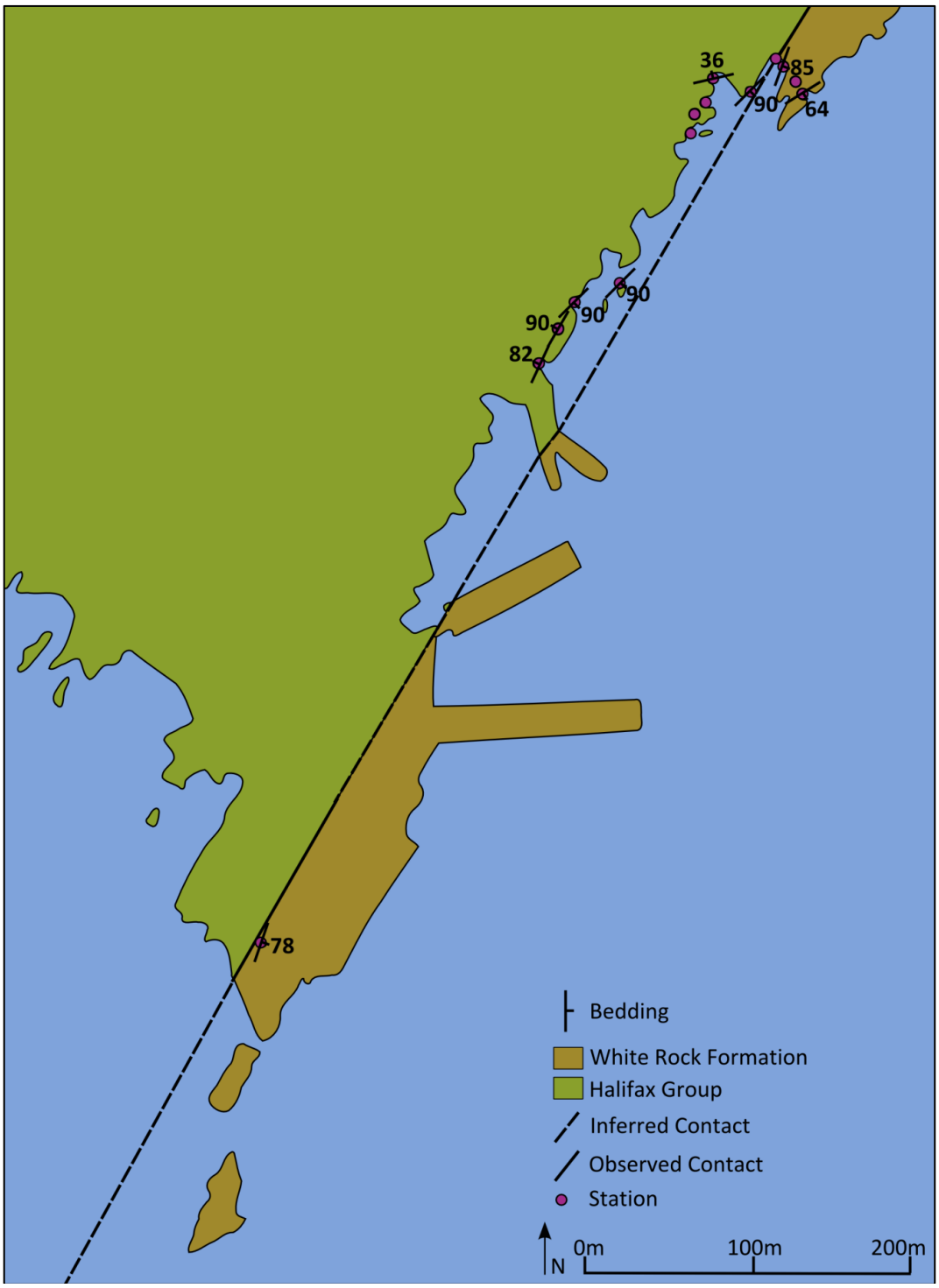

Figure 4.1B: Bedrock geology map with bedding measurements (S_o). Bedding symbol oriented to strike and dip value on dip-direction side.

Intersection lineation measurements were collected at six stations, trending northeast-southwest (with the exception of one measurement). Plunge varied from northeast to southwest and is shallow to moderately plunging (Figure 4.1C).

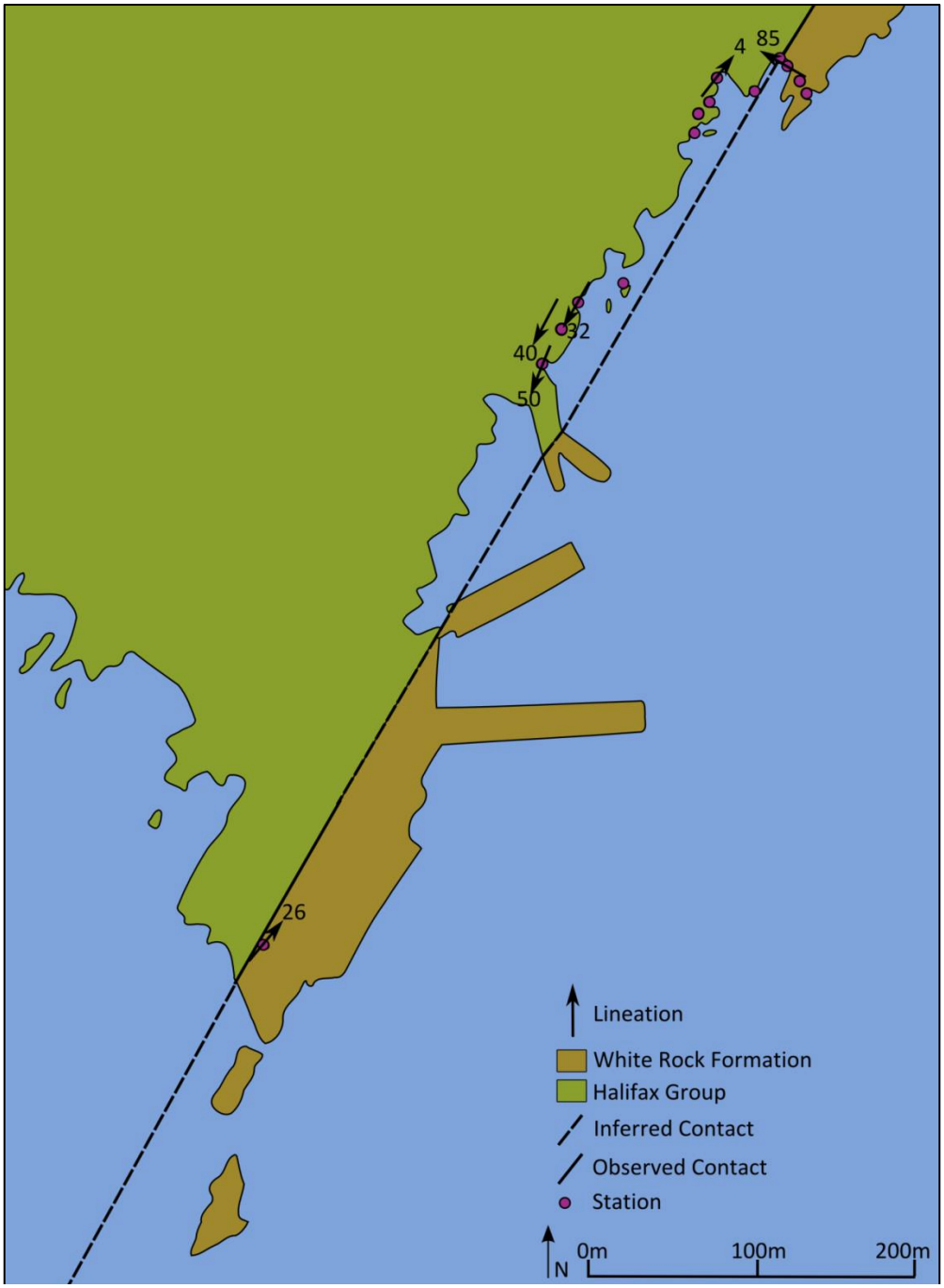

Figure 4.1C: Bedrock geology map with lineation measurements (L_x). Lineation symbol oriented to strike and plunge value on plunge-direction side.

One measurement of a speculated early-stage cleavage (S_{X1}) was recorded very near to the contact and trended northeast-southwest, moderately dipping (Figure 4.1D).

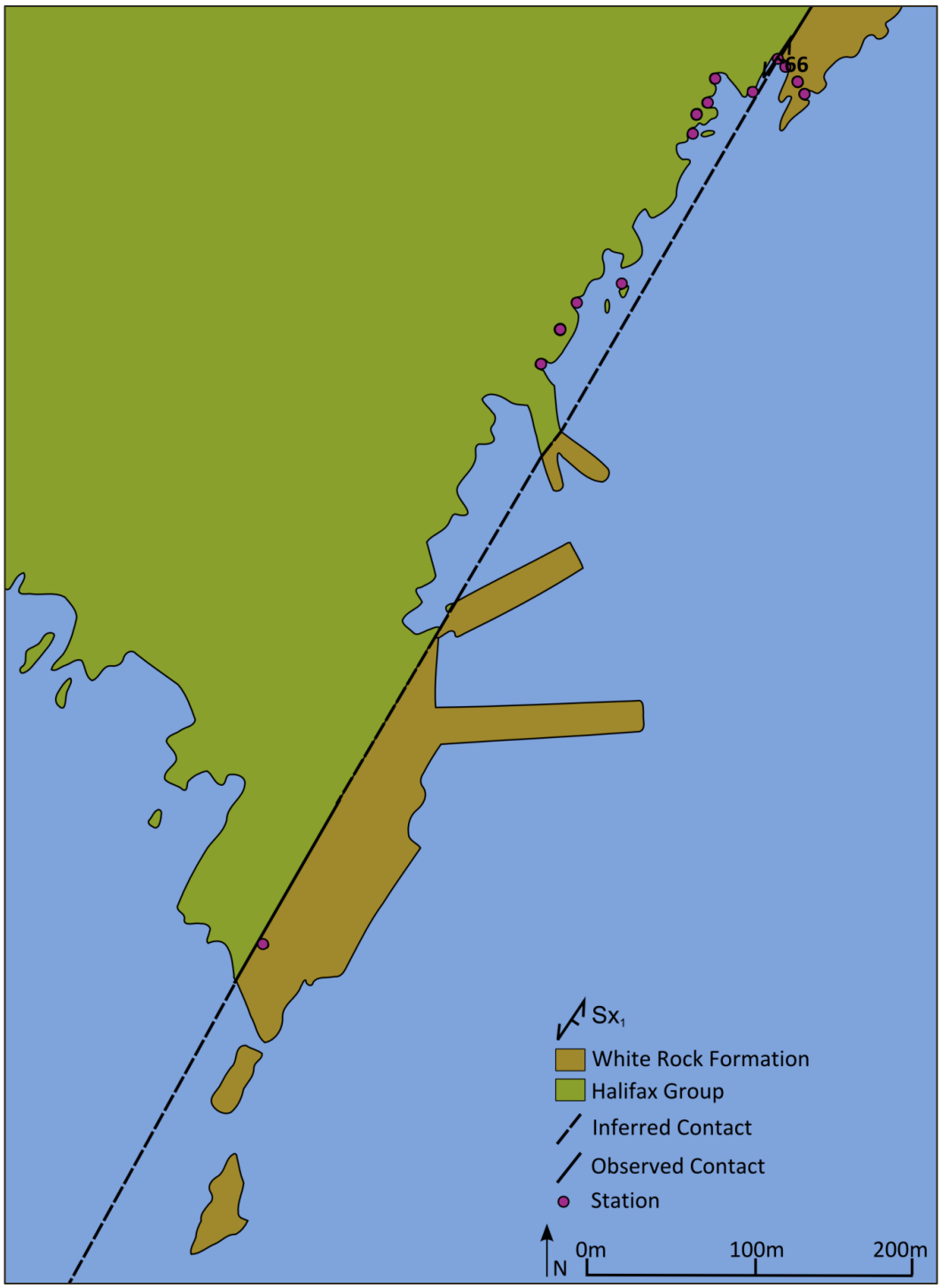

Figure 4.1D: Bedrock geology map with early-stage cleavage measurement (S_{x1}). Cleavage symbol oriented to strike and dip value on dip-direction side.

Speculated late-stage cleavage (S_{X2}) was recorded at thirteen stations throughout the study area. Across the region this cleavage trends northeast-southwest, dipping moderately to steeply southeast (Figure 4.1E).

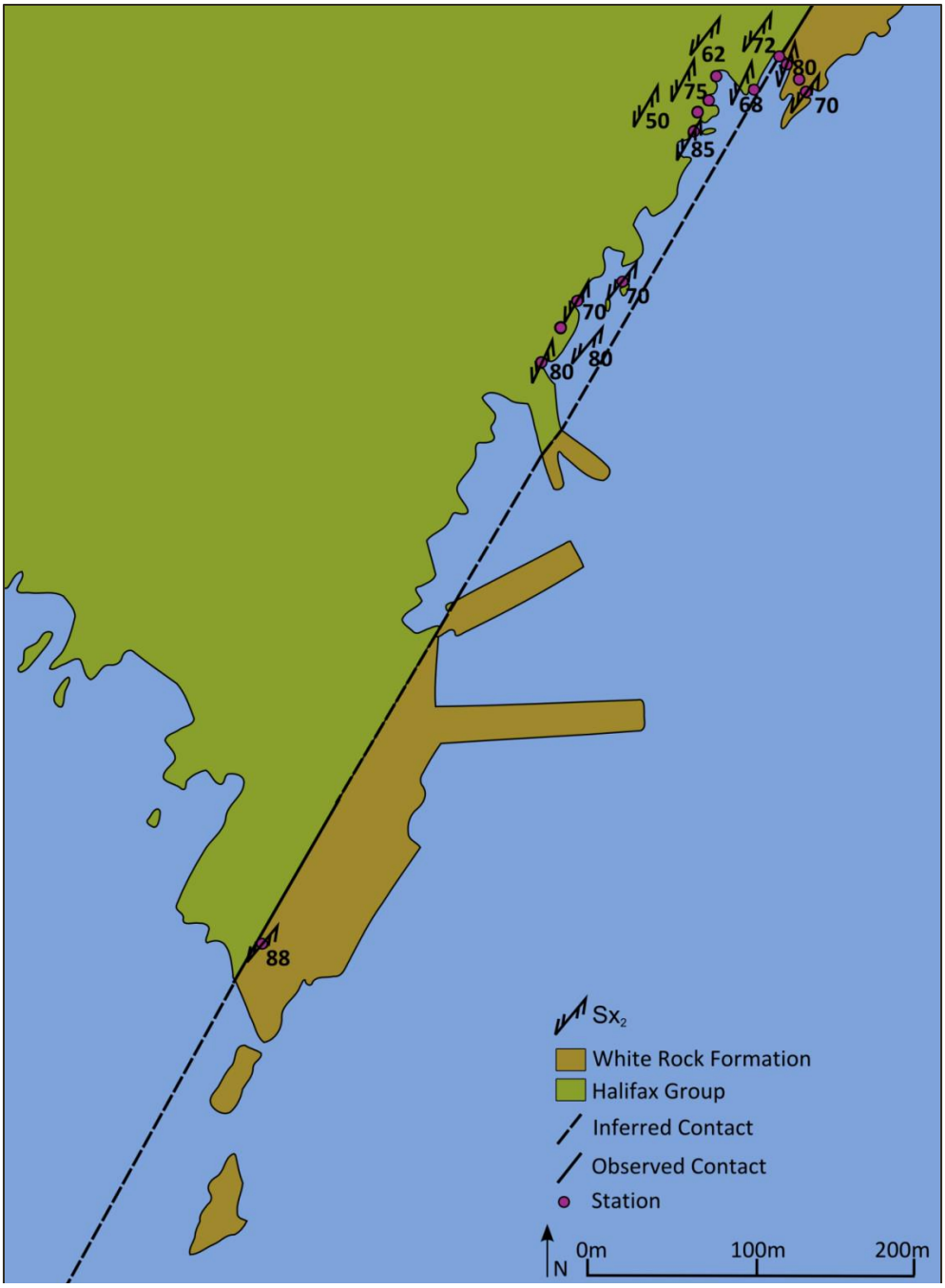

Figure 4.1E: Bedrock geology map with late-stage cleavage measurement (S_{x2}). Cleavage symbol oriented to strike and dip value on dip-direction side. Some measurements migrated off location for increased readability.

4.1 White Rock Formation Quartzite, Greenschist Basalt, and Dacite

The quartzite unit of the White Rock Formation is the furthest unit to the east observed for this study, and is located approximately 10 m east of the contact between the White Rock Formation and the Halifax Group (Figure 4.2A). The quartzite (one of two quartzites at Cape St. Marys) outcrop is approximately 3 m thick and comprises predominantly fine to very fine-grained quartz, with no other macroscopic minerals. The quartzite unit extends further out from the cliff than the greenschist basalt or dacite units of the White Rock Formation due to differential weathering. Quartz veins crosscut the quartzite approximately perpendicular down-dip direction (east) and are 1 to 2 mm wide (Figure 4.2B).

Figure 4.2A: WRF quartzite showing increased resistance to weathering compared to the greenschist basalt unit to the west. Red box indicates location of sample in 4.2B (hammer for scale, 40cm) (Station 013).

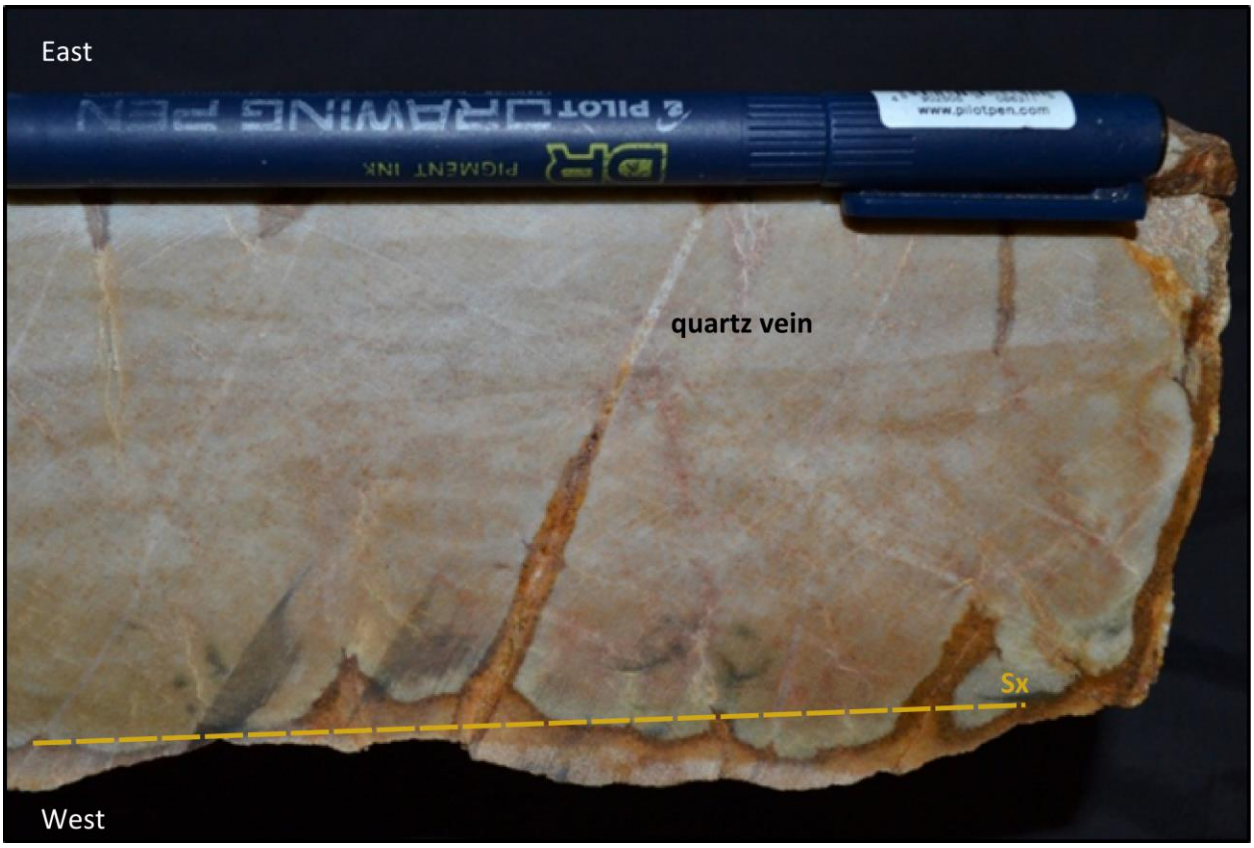

Figure 4.2B: Oriented sample from WRF quartzite, cut perpendicular to S_x cleavage surface. Photo shows weathering rind on edges of quartzite block, and 1-2 mm quartz veins, which occur in the down-dip direction (pole to the quartzite is nearly parallel to dip direction) (pen for scale, 8cm) (Station 013).

Preserved crossbedding is observed in only one location, but is clearly visible, providing information on the younging direction, which is to the east (Figure 4.3).

Figure 4.3: Crossbed preserved in the WRF quartzite, indicating top up to the east (pen for scale, 8cm) (Station 013).

Bedding (S_0) of the quartzite unit strikes to the east-northeast and dips to the east (058/64). A cleavage fabric is visible in the outcrop, and is parallel to S_0, striking to the northeast and dipping to the east (036/70).

The greenschist basalt unit of the White Rock Formation is between the quartzite unit (east) and dacite unit (west), and is located approximately 6 m east of the contact between the White Rock Formation and the Halifax Group. The outcrop of the unit is approximately 4m thick

and the rock is porphyritic, with porphyroclastic phenocrysts of plagioclase and deformed vesicles of calcite (Figure 4.4 & 4.5).

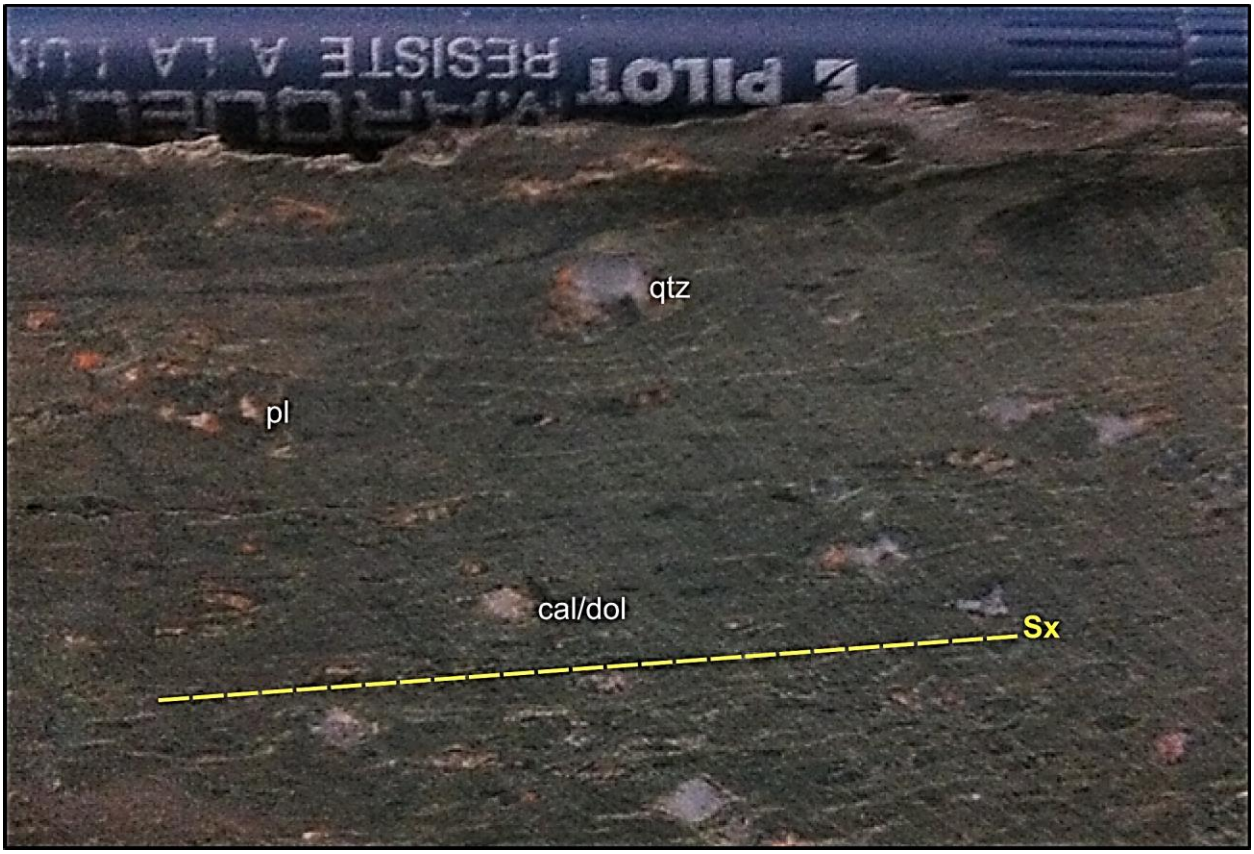

Figure 4.4: Oriented sample from WRF greenschist basalt, cut perpendicular to S_x cleavage surface. Porphyroclasts after phenocrysts of plagioclase and quartz, and calcite vesicles are visible (pen for scale, 6cm) (Station 010).

A cleavage fabric is visible, and is parallel to the cleavage fabric in the quartzite unit, striking to the northeast and dipping to the east (038/72) (Figure 4.5).

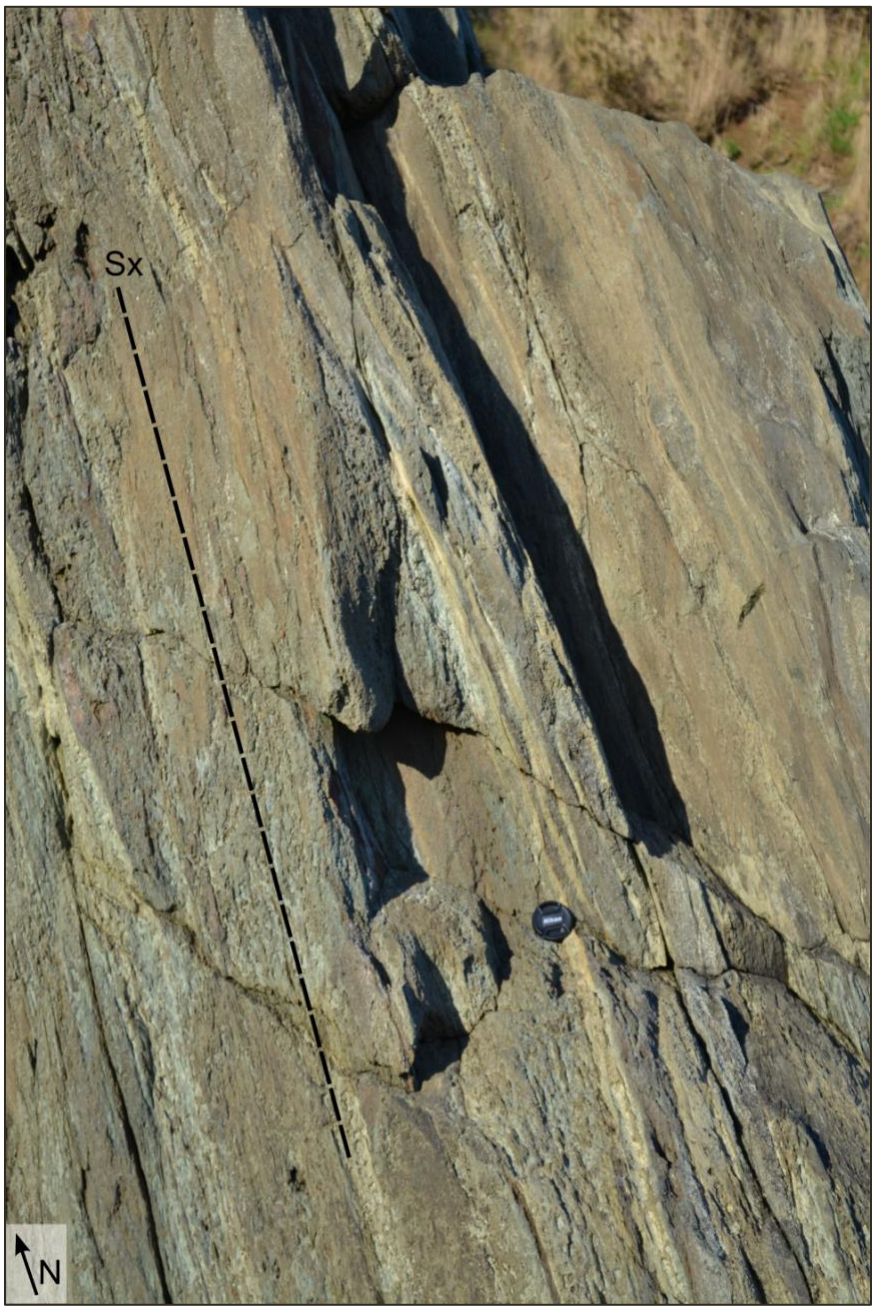

Figure 4.5: Greenschist basalt with S_{x2} cleavage visible (lens cap for scale, 3 cm wide) (Station 010).

The dacite unit of the White Rock Formation is approximately 5 m thick and is located between the greenschist basalt unit to the east and the contact with the Halifax Group slate to

the west. The dacite at outcrop appears pale brown to yellow and is porphyritic, with deformed phenocrysts (lapilli) of plagioclase, quartz, hornblende and biotite. Two cleavage fabrics are visible: the first strikes southwest and dips to the west (216/80) S_{x1}, and the second strikes northwest and dips to the east (034/70) S_{x2} (Figure 4.6). S_{x1} is not commonly preserved in outcrop, and was observed twice only.

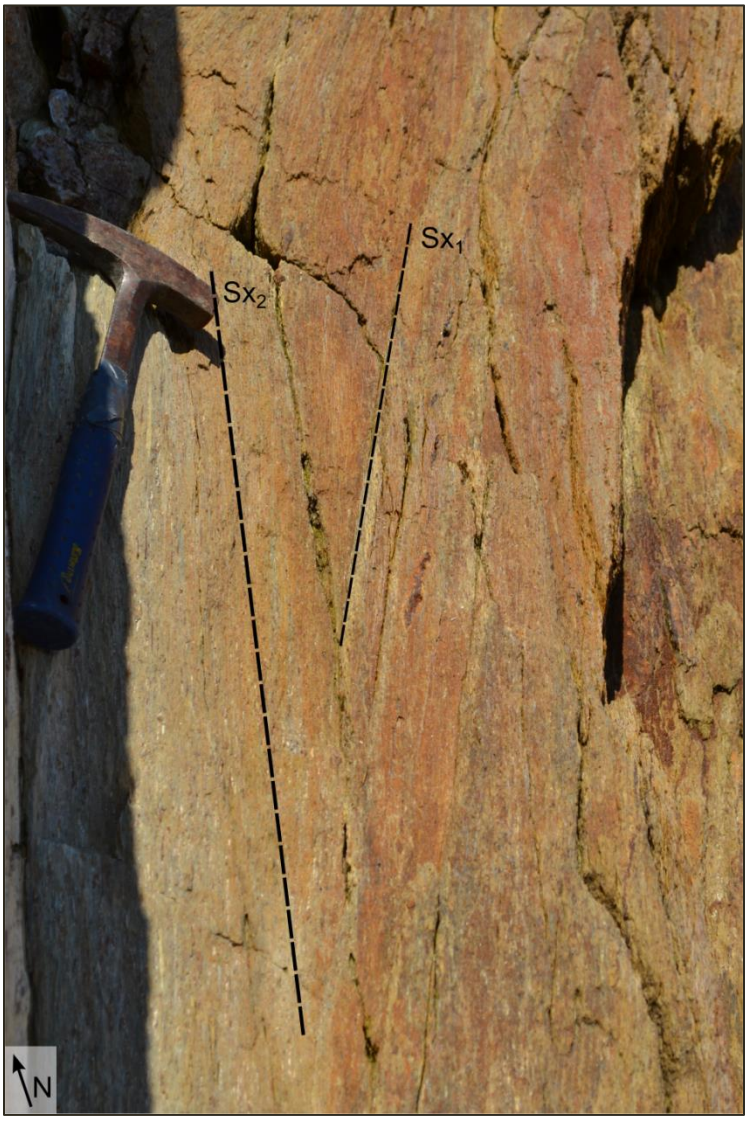

Figure 4.6: WRF dacite with two cleavage fabrics: older (Sx_1) cleavage fabric (216/80) and younger (Sx_2) cleavage fabric overprinting the first fabric (034/70). This older cleavage fabric visible (preserved) in only a few locations on outcrop (hammer for scale, 30 cm) (Station 009).

The first cleavage described has been overprinted almost entirely by the second cleavage, and is infrequently observed. The second cleavage fabric is parallel to those examined in the quartzite and greenschist units of the White Rock Formation, and is parallel to the contact unconformity with the Halifax Group to the west. The earliest cleavage curves into the late cleavage, and therefore sheared in the latest event. Slight variation in the second cleavage is observed as the cleavage

is rarely internally boudinaged (Figure 4.7). The early-stage cleavage developed an internal instability as the rocks continued to deform, and the development of boudin-like structures around this foliation occurred as the late-stage cleavage formed.

Figure 4.7: Internal boudinage of younger cleavage fabric (hammer for scale, 10 cm) (Station 009).

Lapilli are elongated and flattened within the S_2 plane, with long-axes in the down-dip direction of the dacite (Figure 4.8).

Figure 4.8: Down-dip stretching lapilli in S_{x2} plane (dark coloured grains) in dacite, parallel to cleavage fabric (Station 009).

4.2 Bear River Formation Slate

The Bear River Formation of the Halifax Group, comprises interbedded metasiltstone and slate. Overall grain size is very fine-grained to silt-sized, with medium to fine-grained pyrite crystals concentrated in the metasiltstone layers. Bedding (S_0) is variable across strike of the slate, with two zones: (1) bedding steeply dipping (almost parallel to the S_{x2} cleavage fabric) and forming plunging close asymmetric folds, and (2) bedding at a higher angle (further from the S_{x2} cleavage fabric) and forming plunging symmetric folds (Figure 4.9 A-C).

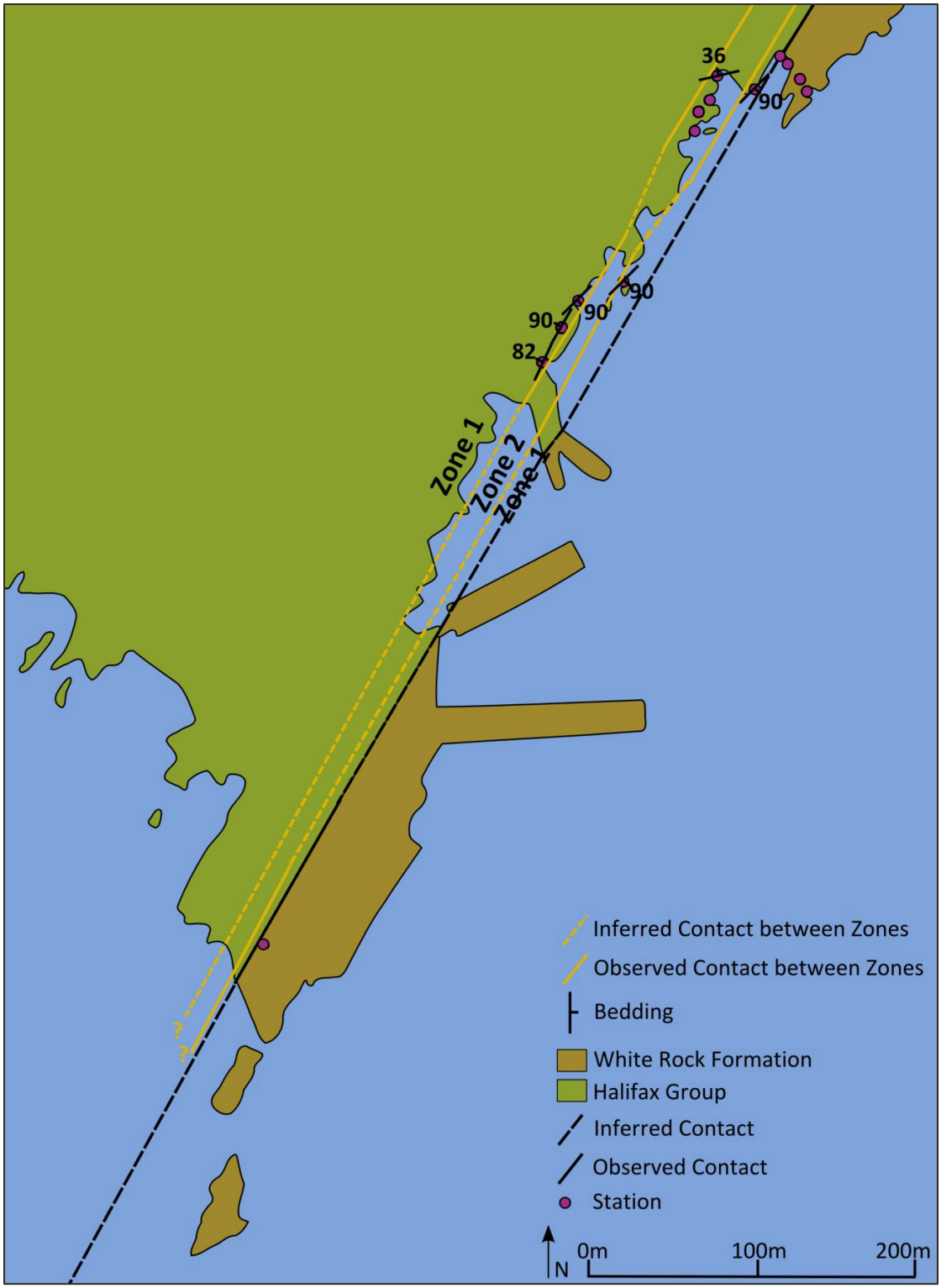

Figure 4.9A: Bedrock geology map showing select bedding measurements observed in the Halifax Group used to define 2 zones observed: Zone 1 - bedding at a high angle (almost parallel to the S_{x2} cleavage fabric) and forming plunging close asymmetric overturned folds; Zone 2 - bedding at a lower angle (further from the S_{x2} cleavage fabric) and forming plunging symmetric folds.

Figure 4.9B: High angle of S_0 to S_{x2} (near transposition) in the first zone in the HG slate (lens cap for scale, 3cm) (Station 004).

Figure 4.9C: Open, subangular to subrounded symmetric plunging folds associated with the second zone in the HG slate; S_{x2} fabric crosscuts S_0 (lens cap for scale, 3 cm) (Station 012).

In both zones, the bedding (S_0) is no longer in its original depositional form and has become deformed and folded, forming the S_{x1} fabric. The S_{x2} cleavage is obvious in outcrop and forms the dominant fabric in both zones of the slate (Figure 4.9B & C). S_{x1} is distinguished from S_{x2} by the relationship between the fabrics – the S_{x1} fabric is crosscut by the S_{x2} fabric (pervasive throughout the study area).

The first zone of the BRF slate is approximately 2 m wide and is where bedding (S_0) is folded, forming the S_{x1} fabric that then forms asymmetric folds (2 to 10 cm across) with thick and thin limbs (Figure 4.10).

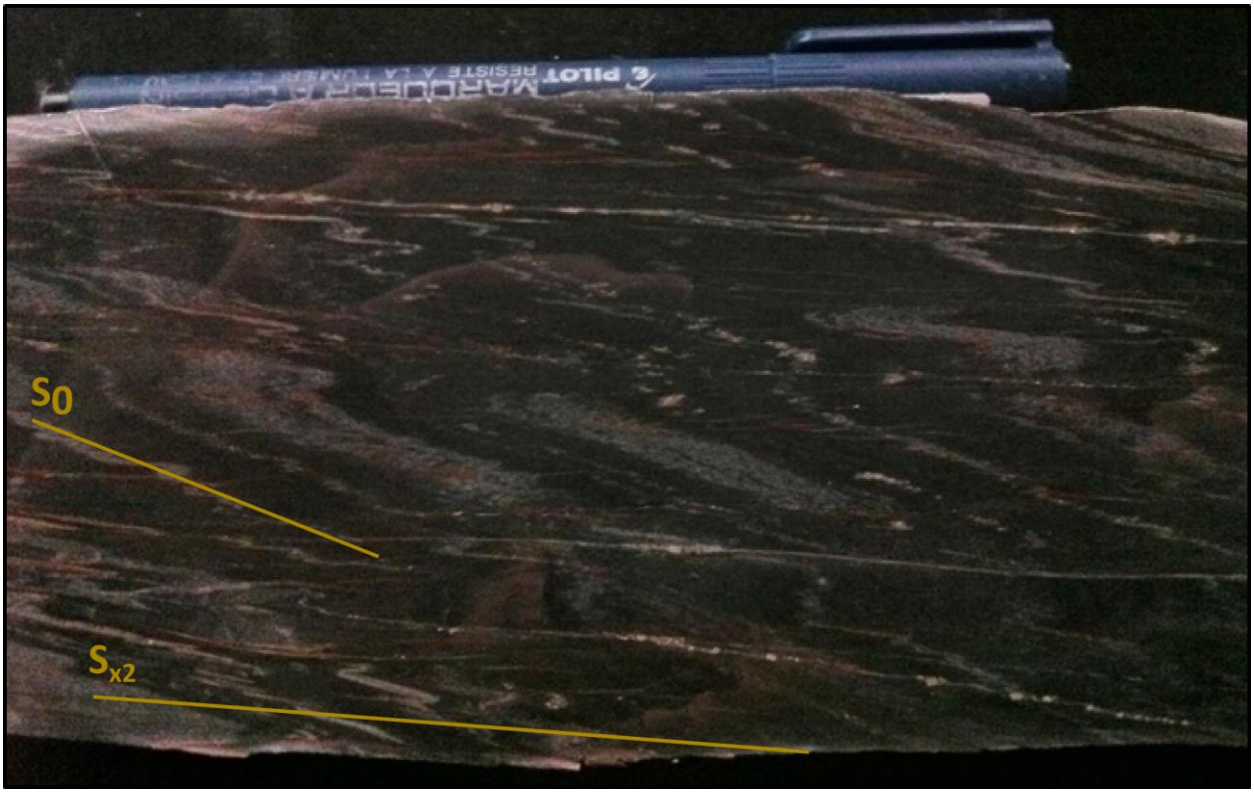

Figure 4.10: Oriented sample cut perpendicular to S_{x2} and S_0, showing asymmetric folds associated with the first zone in the BRF slate (Sample CD_12_005) (Station 008).

Intersection lineation is evident, and represents the intersection of the bedding and cleavage planes; it has a horizontal to moderately dipping plunge that varies along strike (Figure 4.11 A). Stretching lineation is apparent on the cleavage surface in the observed outcrops; it is oriented northeast, dipping east (similar to the stretched lapilli in the WRF dacite) and is formed from quartz tails associated pyrites (concentrated in the metasiltstone layer) (Figure 4.11 B).

Figure 4.11A: Variable intersection lineation between bedding and S_{x2} labelled L and indicated with red lines (lens cap for scale, 3 cm) (Station 008)

Figure 4.11B: Stretching lineation formed from quartz fringes on pyrites labelled with approximation of visible lineation fabric indicated (Station 008).

A critical kinematic feature for this thesis, observed in the first zone of the BRF, was preserved *Arenicolites* burrows. The burrows occur as paired, boudinaged linear structures that are ovoid in cross section; they are subparallel to the S_{x2} cleavage fabric and the stretching lineation (Figure 4.12A & B).

Figure 4.12A: Paired Arenicolites burrows preserved in BRF subparallel to the S_{x2} cleavage fabric; stretching lineation also visible (lens cap for scale, 3 cm) (Station 004).

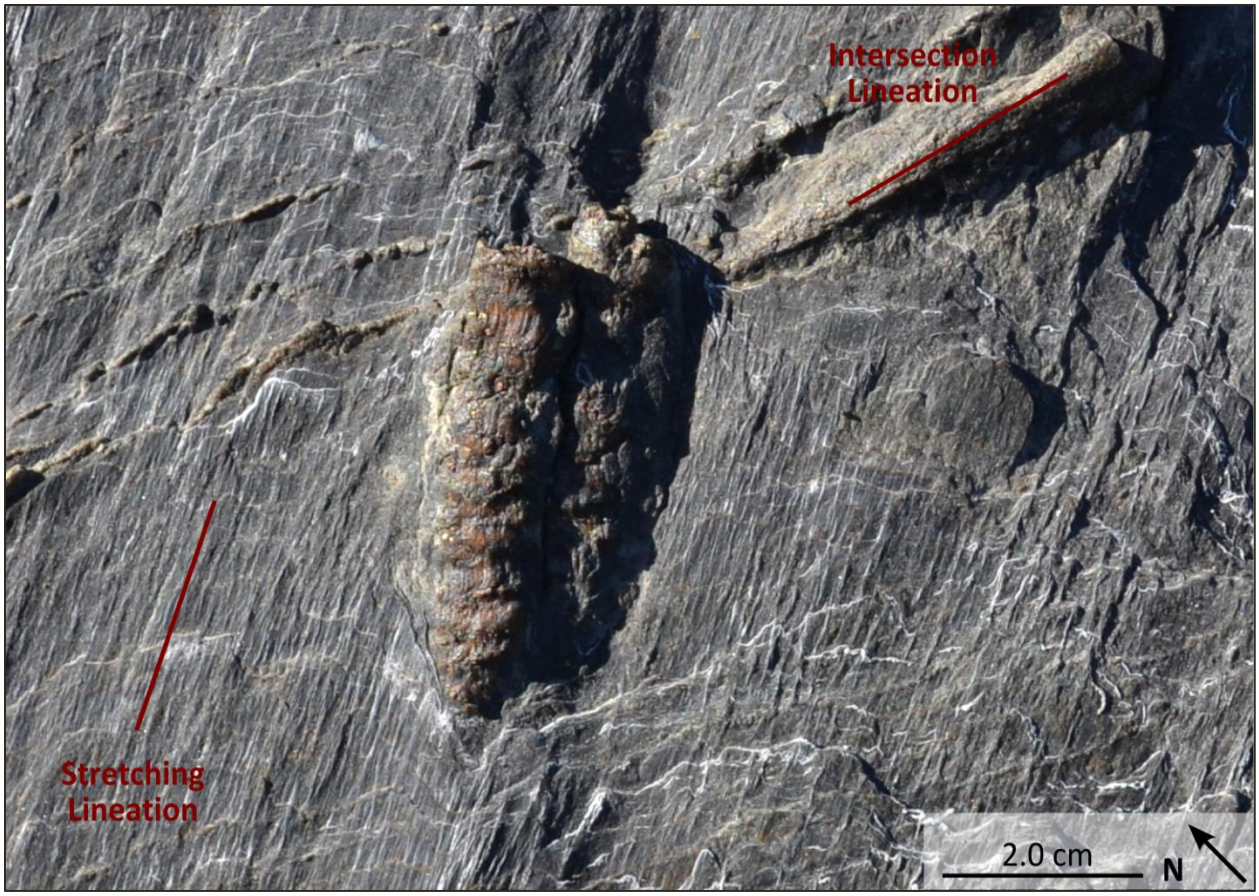

Figure 4.12B: Close up of single burrow showing boundinage of Arenicolites burrows, stretching lineation, and intersection lineation (Station 004).

A sample of this was collected and prepared at the Dalhousie University thin section lab, where a burrow was sliced through to allow the degree of extension and the shear angle (Ψ) to be measured (Figure 3.4B). The degree of extension was measured using the difference between the current length and the original length using the formula $e = (l - l_o) / l_o$; this gave $e = 0.47$, which means the burrows were extended 47% within the S_{X2} plane. The shear angle between the burrow and the bedding was 85^o which was then put in the formula $\gamma \equiv \tan \Psi$, giving a shear strain of 11.43.

Bedding in the second zone is sub-perpendicular to the S_2 cleavage fabric, and forms open, subrounded symmetric plunging folds (Figure 4.9 B). The S_2 cleavage fabric is pervasive throughout and cuts across the S_0 fabric at a nearly perpendicular angle. This second zone is approximately 2-5 m wide, narrower at the northeast end and wider at the southwest end of the study area (Figure 4.9A)

Moving across strike the first zone (2 m wide) is followed by the second zone (2-5 m wide), and is then the first zone reappears (steeply dipping bedding (almost parallel to the S_2 cleavage fabric) and forming plunging asymmetric z-folds folds). The reappearance of the first zone persists northwest beyond the boundaries of the study area (Figure 4.13).

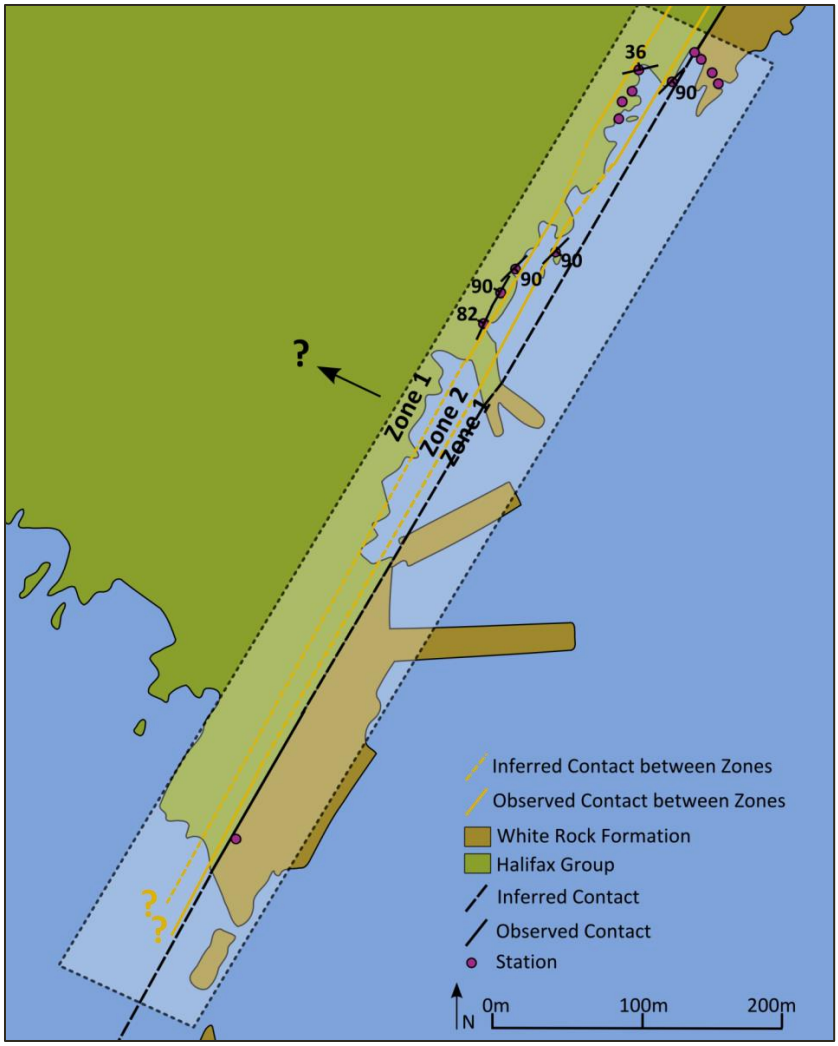

Figure 4.13: Bedrock geology map showing select bedding measurements observed in the Halifax Group used to define 2 zones observed. Study area is indicated with shaded box from oriented NE-SW. The reappearance of Zone 1 continues beyond the boundary of the study area for an unknown distance.

Lineation measurements (intersection lineation of bedding and cleavage) were collected in the BRF slate and the WRF dacite where possible, and then plotted onto a stereonet to determine if the lineation features occurred within a plane (Figure 4.14).

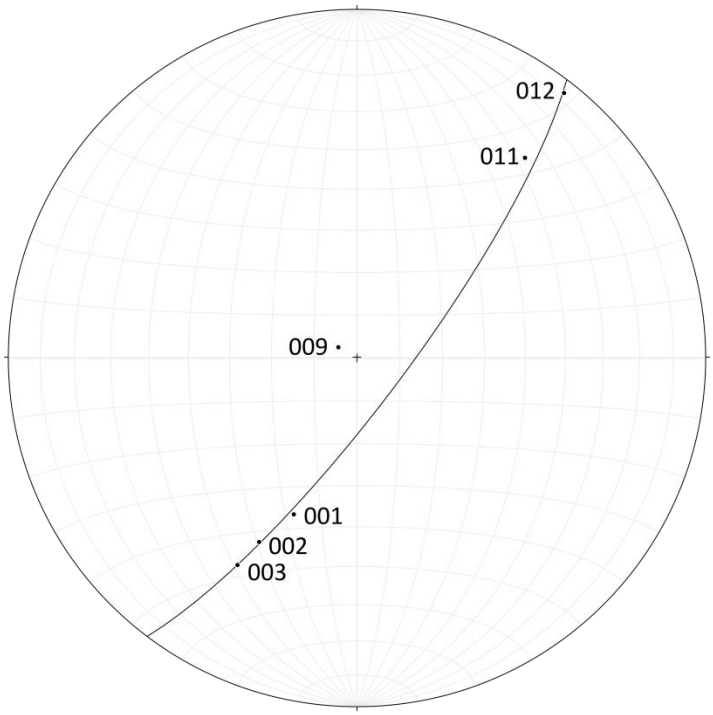

Figure 4.14: Stereonet plot of intersection lineation measurements collected in study area labeled with station location. Note 009 may represent an error in collecting or recording the measurement as it does not follow the trend displayed by the other measurements.

Chapter 5: Petrography Results

This chapter presents petrographic results from the Cape St. Marys samples collected in 2005 and 2012, at the contact between the Halifax Group and the White Rock Formation. Petrography was completed on 18 thin sections in order to:

(1) document mineral assemblages and metamorphic grade of rocks in the study area

(2) determine the effectiveness of microtectonic structures as kinematic indicators for the progressive deformation, defining which structures are associated with each phase of deformation (Neoacadian or Alleghanian)

(3) based the results from (1) and (2) determine if a shear sense is indicated; quantify it where possible.

5.1 White Rock Formation Quartzite

The quartzite samples are fine to very-fine grained with inequigranular grain sizes ranging from 0.1 to 0.5 mm with smaller clastic grains from 0.01 to 0.1mm (e.g. muscovite). Quartzite comprises predominantly polygonal quartz grains (0.1 to 0.5mm), with lesser amounts of muscovite and iron oxides (Figure 5.1).

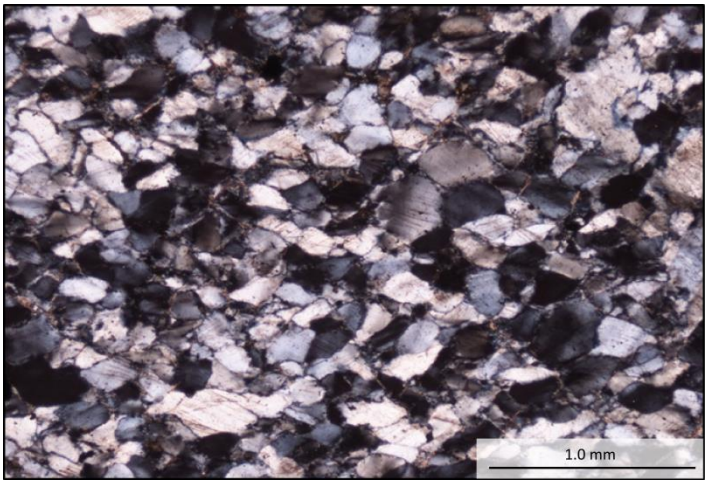

Figure 5.1: WRF quartzite in XPL (5X) showing lamellae and undulose extinction. Note the grains are not very flattened (Sample JF_05_1010, station 013).

Grain boundaries appear sutured and serrated, and recrystallized bulges are observed at the boundaries and cracks of the quartz. Undulose and patchy extinction occur throughout the section examined. Cleavage fabric is defined by quartz grain shape fabric (perpendicular to strike and bedding), striking to the northeast and dipping east (035/68). Deformation lamellae are visible in a large number of quartz grains (Figure 5.2).

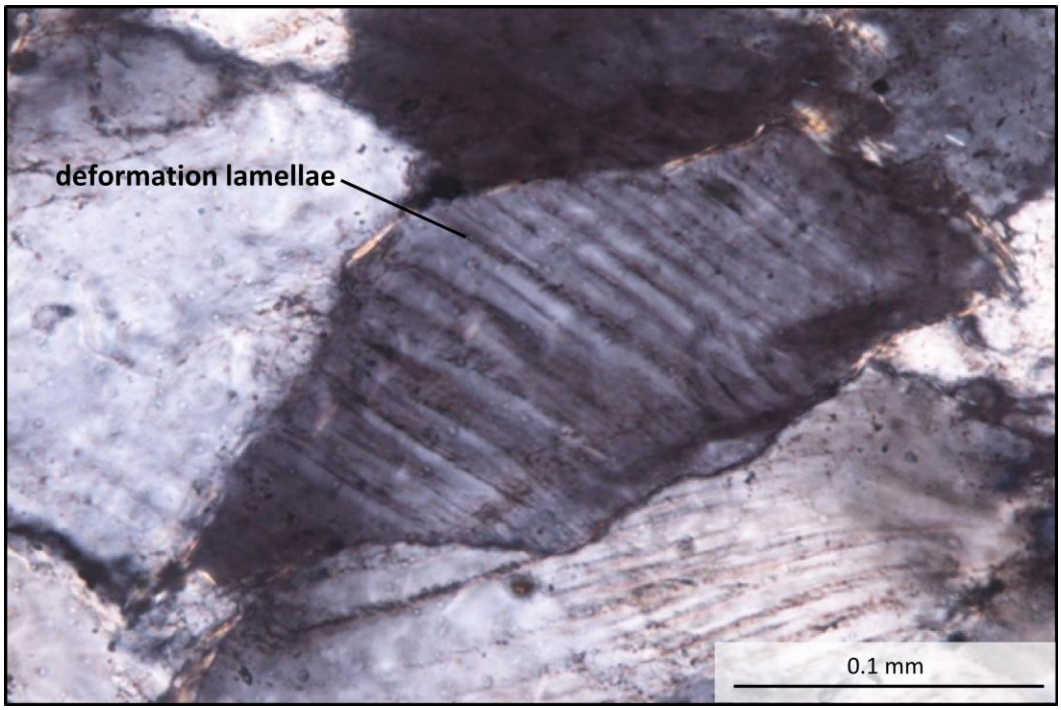

Figure 5.2: Quartz grain from WRF quartzite showing deformation lamellae (XPL 50X, oriented 215/68) (Sample JF_05_1010, station 013).

5.2 White Rock Formation Greenschist Basalt

The greenschist samples are fine-grained and comprise plagioclase, epidote, hornblende (actinolite), chlorite, iron oxides and carbonate. The groundmass comprises epidote, actinolite, iron oxide and chlorite. Plagioclase is frequently present as elongated groups of crystals that pulled apart and are connected with carbonate (Figure 5.3). Chlorite is found in strain shadows

associated with the quartz/carbonate pull-apart structures, but also throughout the matrix. Planar fabric is defined by alignment of grains in the matrix and the porphyroclasts after phenocrysts of plagioclase, carbonate, and minor quartz (Figure 5.4).

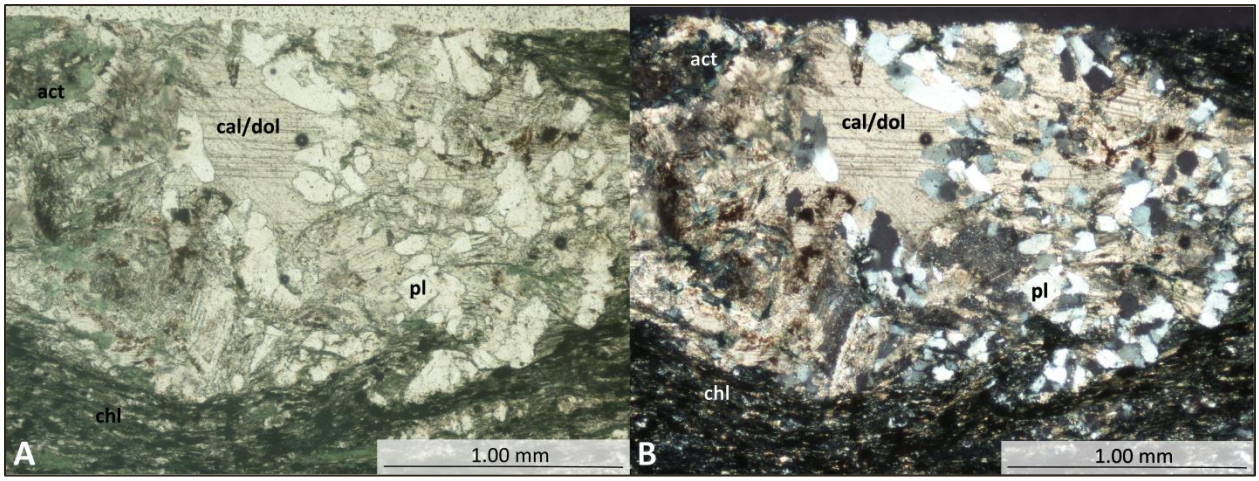

Figure 5.3: (A) PPL section (5X) showing pulled-apart plagioclase that has become filled in with carbonate (calcite and/or dolomite). (B) XPL section (5X) of same sample. Note the fine-grained groundmass comprised of epidote, actinolite, and chlorite (Sample CD_12_009, station 010).

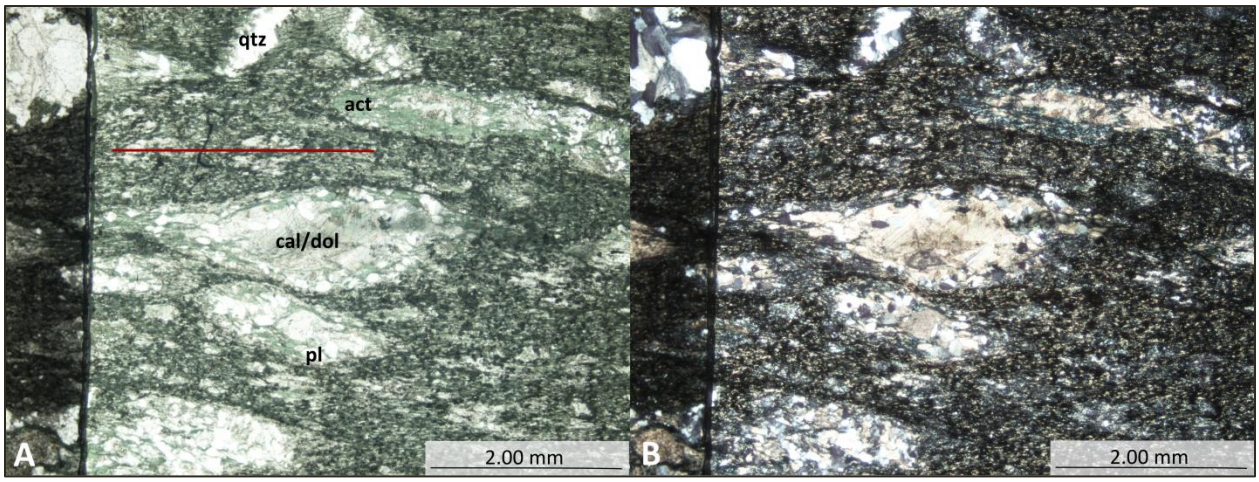

Figure 5.4: Planar fabric of greenschist basalt is observed on the macro-scale (Figure 4.4) and is repeated at the micro-scale (above); it is defined by alignment of the matrix grain and porphyroclasts after phenocrysts of plagioclase, carbonate, and minor quartz (indicated with red line) (A) PPL 2X (B) XPL 2X. (Sample CD_12_009, station 010)

5.3 White Rock Formation Dacite

The dacite samples contain porphyroclasts in a fine-grained matrix, with inequigranular grain sizes from 0.1 to 0.5 mm and smaller clastic grains less than 0.01 to 0.1mm (muscovite, biotite, plagioclase, quartz, and iron oxide). Groundmass comprises predominantly microcrystalline quartz, plagioclase, hornblende, muscovite, biotite, pyroxene, and glass. Porphyroclasts of plagioclase and quartz are frequent, ranging in size from 0.5 to 1.5mm, and are often highly fractured (Figure 5.5A &B). Plagioclase porphyroclasts show polysynthetic twinning. Planar fabric is defined by alignment of grains in the matrix, porphyroclasts, and the pressure solution cleavage.

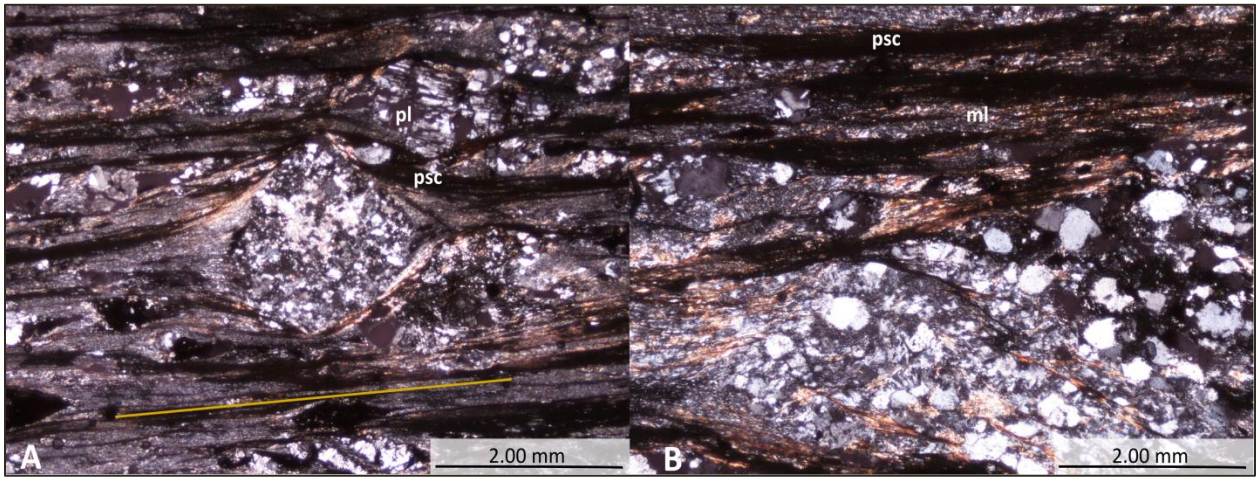

Figure 5.5: (A) Porphyroclasts of highly fractured quartz, plagioclase, and iron oxides. Pressure solution cleavage observed terminating against porphyroclasts boundary. Planar fabric observed in WRF greenschist (Figure 5.4A) also observed in WRF dacite (indicated with yellow line on thin section image). (B) Another porphyroclasts, with pressure solution cleavage (psc) tracing into the porphyroclast. Microlithons (ml) of mica are more visible and are aligned to a different angle than the planar fabric (Sample CD_12_003a, station 009).

Pressure solution cleavage is defined by dark bands (parallel to S_{x2} measurement from structure work), striking to the northeast and dipping east (036/72) (Figure 5.5). Microlithons of

quartz, plagioclase, hornblende, muscovite, biotite, pyroxene, and glass occur between the pressure solution bands. Microlithons appear to be aligned along a different cleavage plane (approximately parallel to S_{x1} measurement from structure work) than then pressure solution bands surrounding them (Figure 5.5).

5.4 Bear River Formation Slate

The slate samples are fine to very-fine grained and inequigranular with grain sizes from 0.1 to 3.0 mm and a microcrystalline groundmass. Groundmass comprises predominantly quartz, muscovite, and iron oxide, with crystals often too small to determine composition under the petrographic microscope. Porphyroblasts of pyrite are common, and occur as core-objects with quartz dominant strain fringes (carbonate is occasionally found in the strain fringe) (Figure 5.6). Pressure solution cleavage is also present in the HG slate (as in WRF dacite and greenschist basalt), and is frequently terminated where it intersects fringe structures. Planar fabric parallel to S_{x2} is present and is defined by the alignment of grains in the groundmass, porphyroclasts-based fringe structures, and pressure solution cleavage.

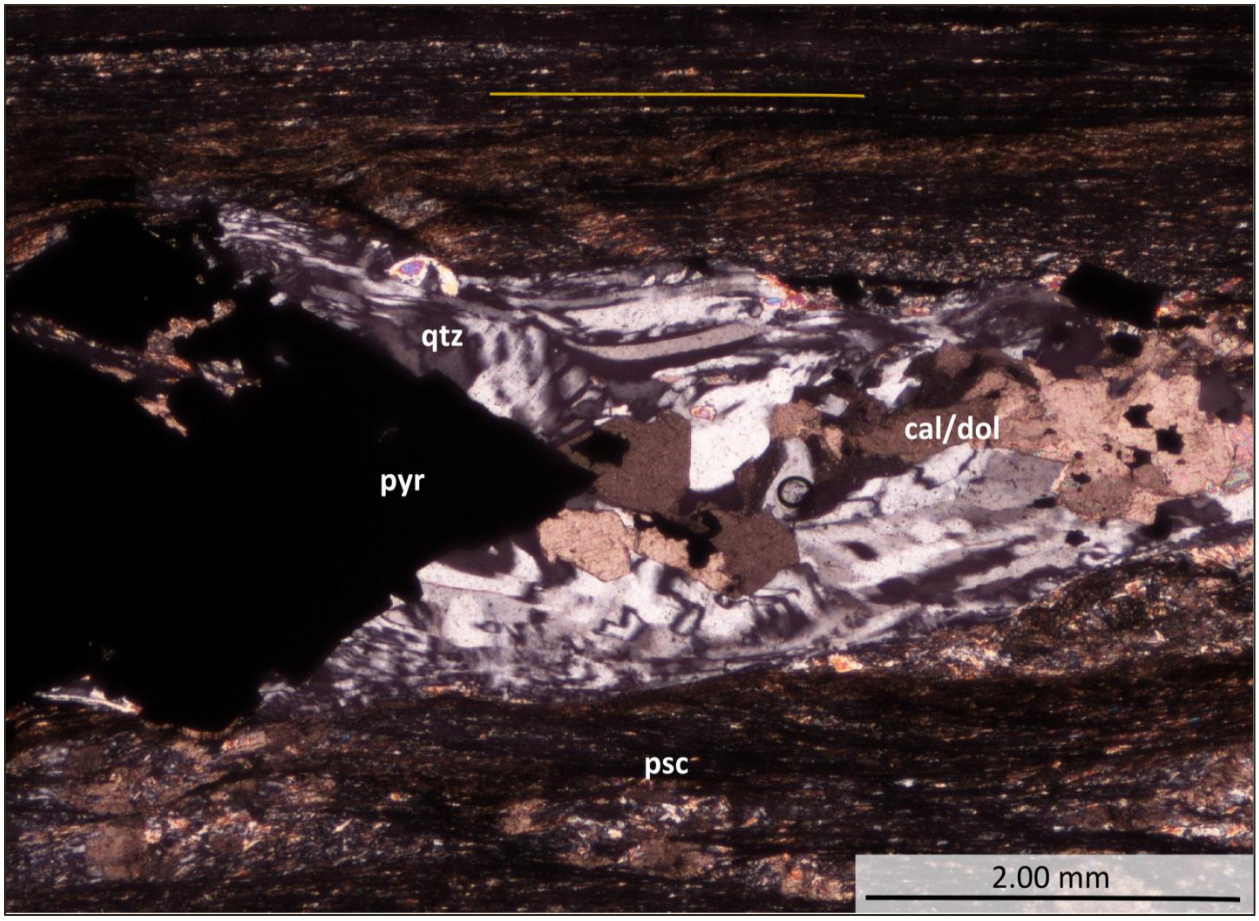

Figure 5.6: Pyrite porphyroblast as core-object with quartz and carbonate strain fringe. Pressure solution cleavage (psc) is observed throughout all BRF thin sections; combined with aligned grains in ground mass and fringe structures defines planar fabric parallel to S_{x2} (indicated with yellow line on thin section photo) (XPL 5X) (sample CD_12_001b, station 014).

The pyrite core-objects commonly cluster together in groups, so the associated quartz and carbonate strain fringes are in contact with each other (Figure 5.7).

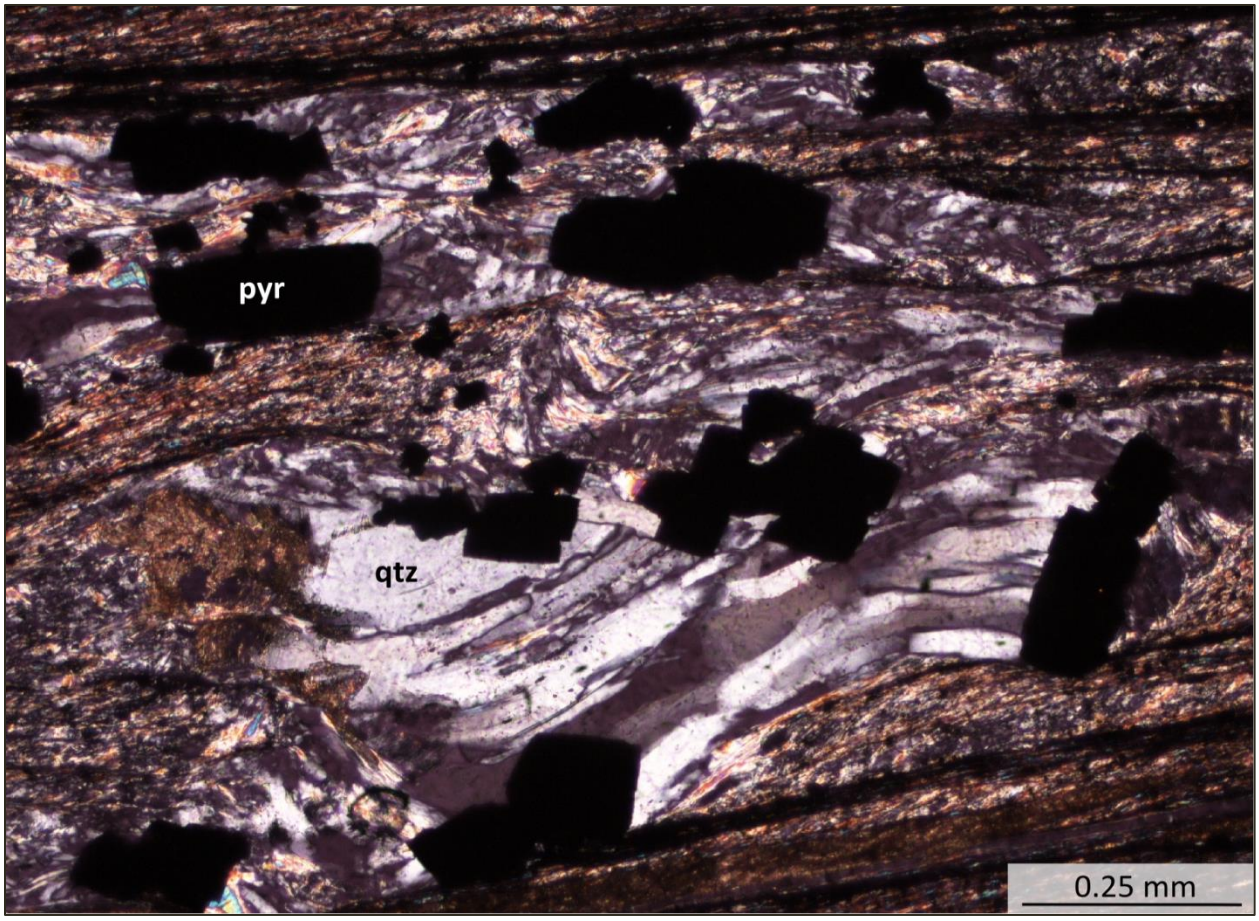

Figure 5.7: Cluster of pyrite porphyroblasts and quartz strain fringes in contact and interfering with each other during deformation (XPL 10X) (sample CD_12_001a, station 014).

The quartz grains in the strain fringes have deformation bands parallel to the quartz grain (zones of approximately uniform extinction which grade over a short distance to into other sectors with slightly different orientation) and/or have entirely recrystallized (Passchier & Trouw, 2005). A sharp change in the orientation of the quartz crystals (with respect to either side of the linear feature) is occasionally observed in the quartz fringe (Figure 5.8). Occasionally pyrite core-objects are fragmented (identified by corresponding edges) and quartz fringes occur in between parts of the broken rigid crystals.

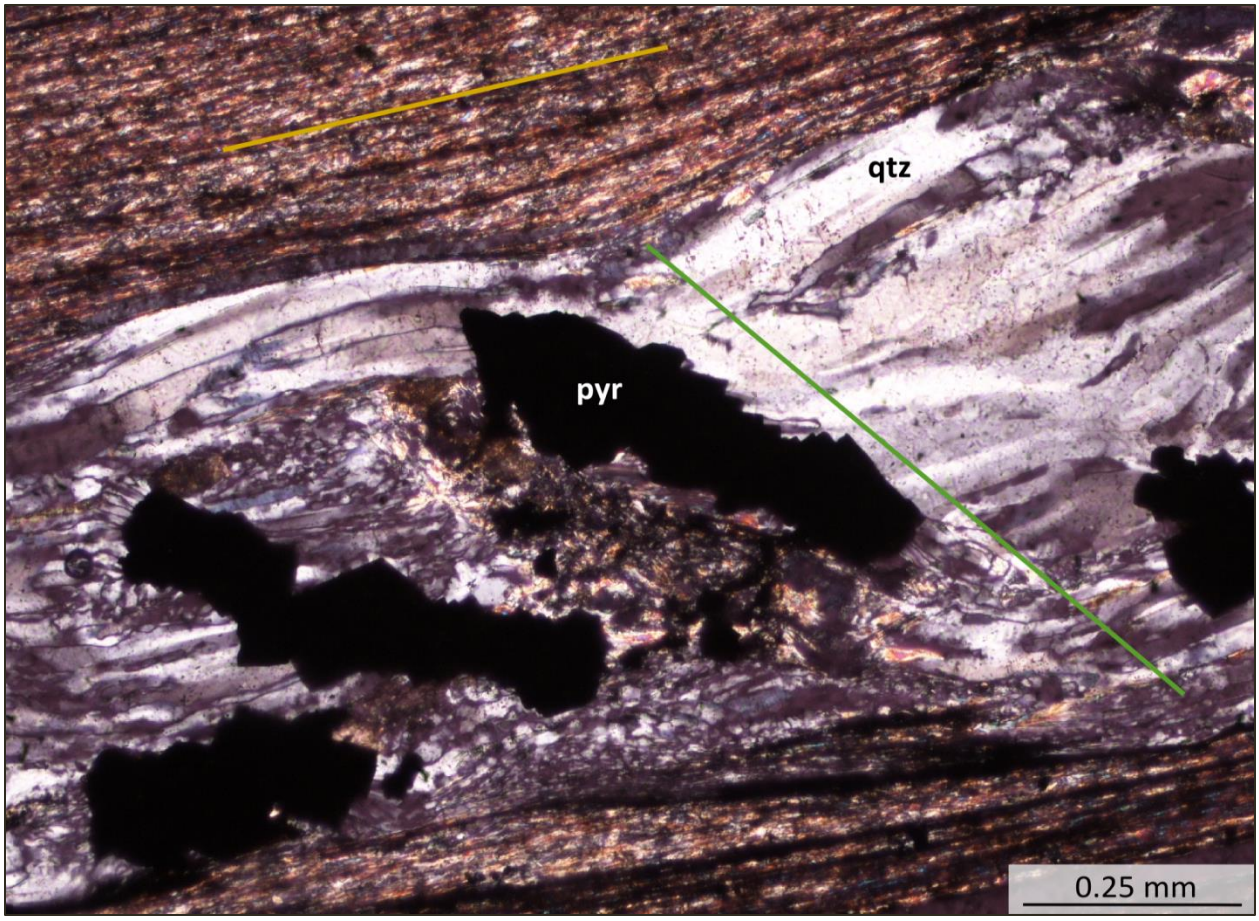

Figure 5.8: Elongated pyrite grain with displacement-controlled quartz fringe. Sharp change in the orientation of the quartz fringe occasionally observed (green line); this change is at a different angle (almost perpendicular) to the planar fabric (yellow line) (XPL 10X) (sample CD_12_001a, station 014).

Pyrite core-objects and their corresponding strain fringes were analyzed from four thin sections for several features: grain shape, location (group or isolated), dimension (equal or elongated), direction of deformation (dextral, sinistral, or unknown), recrystallization of fringe, and fringe growth (face or displacement-controlled) (summarized in Table 1, full detailed results in Appendix I). Total number of fringe structures for each sample is given; there are a total of 219 fringe structures that were analyzed. The grain shape is defined as either elongated (one dimension of core-object is notably longer than the other) or equidimensional (dimensions

of the core-object are nearly equal to each other). The fringe structures were observed in one of three positions: as part of a group, on the edge of a group, or isolated. It was important to note the position as the strain fringes and core-objects could have interfered with other strain fringes and core-objects during deformation, effecting the crystal growth and shear sense direction. The shear sense direction was observed for each strain fringe as a kinematic indicator of progressive deformation in the rocks; it was determined by which direction the host rock would be required to shear to produce the observed structure and was recorded in one of three states: dextral, sinistral, or unknown.

Table 1: Summary of analysis completed on Halifax Group Slate pyrite core-objects and their associated strain fringe.

Sample	Number of Fringe Structures	Grain Shape		Position			Shear Sense Direction		
		Elongated	Equal	Group	Edge of Group	Isolated	Dextral	Sinistral	Unknown
CD_12_001a	76	44	32	45	8	23	18	28	30
CD_12_001b	55	24	31	35	16	4	8	22	25
CD_12_004a	37	26	11	25	5	7	10	16	11
CD_12_004b	51	22	29	17	14	20	4	26	21
Total	219	116	103	122	43	54	40	92	87
%	100	52.97	47.03	55.71	19.63	24.66	18.26	42.01	39.73

The position of the grains analyzed were recorded for each thin section to determine if there was a correlation between the position on the short or elongated limb of the asymmetric z-folds and one of the features analyzed (slides were analyzed with west side-up as independent reference direction) (see Appendix II for full thin section scans).

Chapter 6: Discussion

In the White Rock Formation, the quartzite yielded a (single) crossbed, providing information that the unit is top-side up towards the east. The base of the crossbed is parallel to the S_{x2} cleavage fabric that is pervasive across the study area. Observations of the unconformity and the S_{x2} fabric showed that the S_{x2} cleavage fabric is parallel to the unconformity contact with the Halifax Group. No evidence for a discrete fault (slickenlines, fault gouge, breccia, etc.) in the Halifax Group slate or the White Rock Formation units was observed.

In thin section, the most noticeable feature of the quartzite deformation lamellae in the quartz grains, indicating the quartz had reached a sufficient temperature that it was ductile enough to allow the lamellae to form but only just enough to allow dislocations. The lamellae likely formed by dislocation creep; dislocation creep can occur over a wide range of temperatures (1) bulging recrystallization at low temperature, (2) subgrain rotation recrystallization at intermediate temperature, and (3) grain boundary migration recrystallization at high temperature (Passchier & Trouw, 2005). The temperature zone for bulging recrystallization is 270-420°C, while subgrain rotation recrystallization occurs from 390-530°C (Stipp, et al., 2002).

Petrologic evidence (mineralogy) is normally used to determine the approximate temperature experienced by the rock based on the minerals and textures observed; however the composition of the quartzite is unable to provide constraints on the metamorphic grade as it does not contain mineral grains of sufficient size (beyond quartz) to confidently determine this. The WRF greenschist basalt is in direct contact with the quartzite, therefore it is

reasonable to infer that the units have undergone similar pressure-temperature conditions. The mineralogy of the greenschist basalt (plagioclase + epidote + actinolite + chlorite) is a definite mineral assemblage for a greenschist mafic rock, and is of the medium pressure/temperature (P/T) series (pressures of 0.1-0.9GPa and temperatures of 300-500°C) (Figure 6.1) (Winter, 2010). When temperature constraints on quartz deformation are interpreted with the microstructures and mineralogy observed, deformation lamellae in the quartz are likely to have formed by subgrain rotation at temperatures from 390-500°C (Figure 6.2).

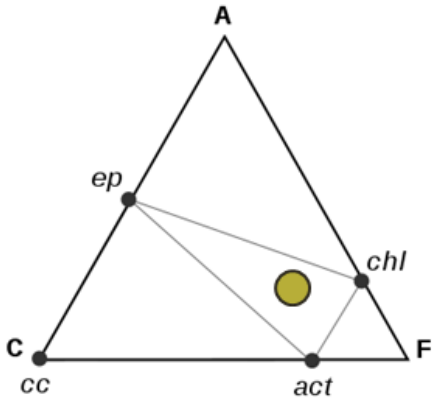

Figure 6.1: ACF (aluminium-calcium-iron) diagram showing phase equilibrium for greenschist facies. Approximate plot location for WRF greenschist basalt shown.

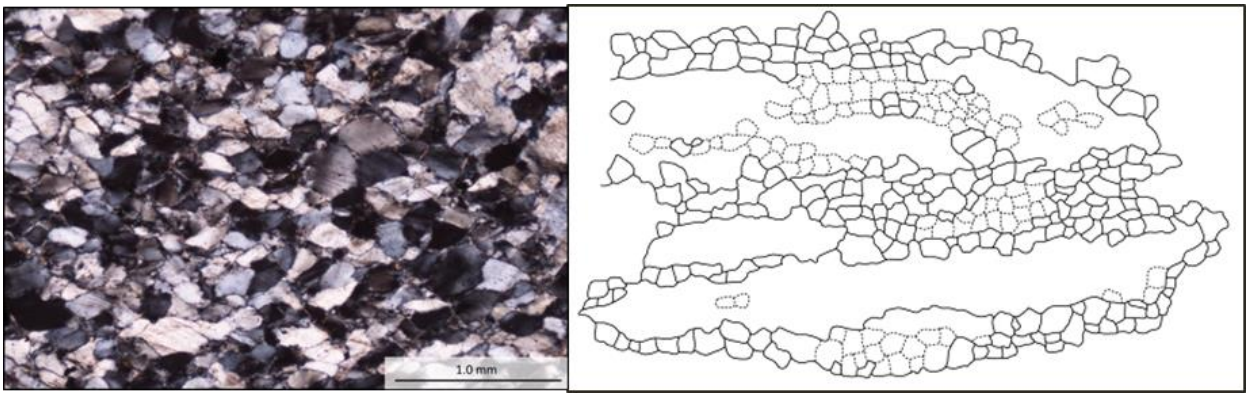

Figure 6.2: XPL image of WRF quartzite thin section (left) showing texture of quartz grains; diagram of subgrain rotation texture (Stipp, et al., 2002).

The WRF greenschist basalt would have originally comprised olivine + plagioclase ± pyroxene ± quartz. When the rocks were exposed to medium pressure and temperature (pressures 0.1-0.9GPa and temperatures 300-500°C) the minerals metamorphosed through a series of reactions. These reactions led to the observed mineralogy of plagioclase + epidote + actinolite + chlorite + quartz + iron oxides. The conditions required for subgrain rotation and medium P-T greenschist facies metamorphism overlap to constrain pressure and temperature to 4-7kb and 420-500°C (Figure 6.3). Carbonate was also observed in the WRF greenschist but was not part of the original mineralogy; its formation would have been from interaction with CO_2 dissolved in hydrothermal fluids.

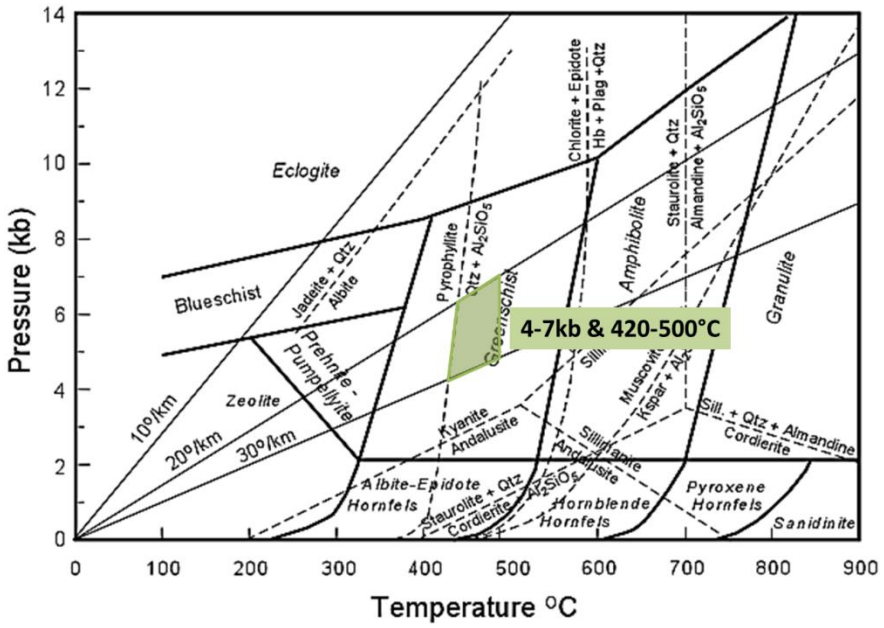

Figure 6.3: Pressure-Temperature conditions causing greenschist facies metamorphism in rocks at CSM (Winter, 2010).

Carbonate (calcite and dolomite) is observed in the Halifax Group slate, and the White Rock Formation dacite and greenschist. Calcite and dolomite filled fractures and voids/cavities as the rocks were extended in the plane of the S_{x2} fabric, and would have been precipitated from fluids that flowed through and interacted with the rocks. CO_2 would have been dissolved

in hydrothermal fluids, but becomes immiscible when temperature falls below approximately 300^{o}C and begins to precipitate onto surfaces. As evidenced by the temperatures reached for the greenschist facies metamorphism and the formation of deformation lamellae by bulging recrystallization, temperatures did exceed 300^{o}C and then cooled through this allowing for the precipitation of the carbonate.

The WRF dacite unit contains lapilli that are stretched down-dip, which indicates the direction of extension in the rocks is within the planar surface represented by the lapilli – the S_{x2} cleavage fabric (034/70). The burrows observed in the Halifax Slate group have become rotated into the S_{x2} cleavage plane and also show extension (as boudinage) in the same direction as the lapilli, supporting the conclusion that extension is in the S_{x2} cleavage plane (plane strain with 2D pure shear). The burrows would have rotated during the Neoacadian and Alleghanian phases, and we are not able to determine how much rotation can be credited to each at this time; however in the preserved Neoacadian folds they are likely to have been at a high angle. Based on earlier research, down-dip boudinage and extension are not characteristics typically associated with the Neoacadian phase, but hinge parallel extension is occasionally noted; down-dip boudinage and extension is associated with the Alleghanian, so the extension is likely from the Alleghanian phase.

As discussed in Chapter 4 for the Halifax Group slate, there were two distinct zones of structures, which were defined based on the angle between the bedding (S_0) and the dominant S_{x2} cleavage fabric. In the first zone bedding is steeply dipping (almost parallel to the S_{x2} cleavage fabric) and exhibits asymmetric overturned folds; in the second zone bedding is

subperpendicular to S_{x2} cleavage fabric and exhibits plunging subrounded symmetric folds. The first zone is termed the zone of Near Transposition due to S_0 at a steep dip and almost parallel to S_{x2}. The second zone is termed the zone of Preserved Neoacadian Folds as S_0 is still visible with the S_{x1} fabric preserved (as subrounded folds crosscut by S_{X2} cleavage). The S_{x1} folds are attributed to the Neoacadian, as the limbs are equal thickness, formed from buckle-style folding which is consistent with Neoacadian fold geometry. This zone would have involved transposition of the Neoacadian fabric with the Alleghanian fabric (as with the zone of Near Transposition) but, for reasons unknown, some S_{x1} fabric was preserved.

The preserved burrows were also used to provide information on the shear angle between the burrow and the bedding, which was 85^{o}; this value was then used to determine a tensor shear strain of 11.43. The shear strain of 11.43 translates to 1143m of displacement for every 100m across the transposition zone.

Intersection lineation measurements were plotted onto a stereonet, and showed that five out of six of the collected values plotted onto a single plane (037/79) (Figure 6.4). The intersection lineation was that of the bedding and the S_{x2} cleavage fabric. The points did not plot as a cluster, but as a trend, showing the deformation that formed the lineation was progressive and did not result from a single (rapid) event.

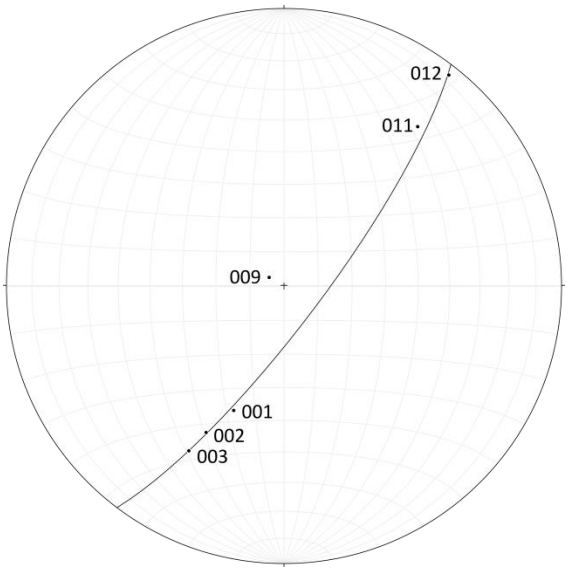

Figure 6.4: Stereonet plot of intersection lineation measurements collected in study area labeled with station location.

Pressure solution cleavage was observed in the White Rock Formation quartzite, greenschist basalt, dacite and the Halifax Group slate. Pressure solution cleavage is localised dissolution of material induced by enhanced solubility of solids in response to the presence of a differential stress field, in this case where the grains were in contact along surfaces at a higher angle to the instantaneous shortening direction (Passchier & Trouw, 2005). Evidence of differential stress are the formation of two cleavage fabrics (S_{x1} and S_{x2}) that are near perpendicular, and the extension of the lapilli in the dacite and preserved *Arenicolites* burrows in the slate. There would have been a reduction in volume where the pressure solution cleavage occurred (dark bands), and the material would have diffused to sites of lower solubility by solution transfer. This material was probably the source for the fringes on the pyrite core-objects as the strain fringes grew. According to previous work, pressure solution cleavage is not generally a characteristic associated with the Neoacadian, but is found readily in

rocks approximately 1 km to the west of the unconformity (still in Halifax Group slate) that have been dated using $^{40}Ar/^{39}Ar$ methods as Alleghanian in age. This it is reasonable to consider the pressure solution cleavage observed in the study area to be of Alleghanian age (S_{x2} – Alleghanian age?). Microlithons between the pressure solution cleavage may have preserved previous fabrics in the rock (S_{x1} - Neoacadian age?).

The pyrite grains in the Halifax Group slate have strain fringes of quartz (rarely with carbonate), which are isolated or grouped. The fringes are parallel to the S_2 cleavage, and are displacement-controlled and/or face-controlled. The more elongate the pyrite core-object, the less vorticity demonstrated. A sharp change in the orientation of the quartz crystals was observed in some of the fringes, partitioning the quartz strain fringe into earliest-formed and latest-formed quartz; and indicates a change in the direction of the deformation at this boundary. The earliest-formed quartz in the strain fringes (furthest from the pyrite core-object) is potentially associated with the Neoacadian phase deformation (400-370 MYA); the latest-formed quartz (in contact with the pyrite core-object and between the pyrite and the sharp change boundary) is potentially associated with the Alleghanian phase deformation (325-260 MYA).

The asymmetric folds of the zone of Near Transposition are visible in thin section; forming the asymmetric folds in the younger fabric required shearing the Neoacadian phase buckle folds during the Alleghanian phase (Figure 6.5). The orientation of the z-folds in the slate suggests that if the White Rock Formation was not present to the east, an antiform would be

present. The intersection lineation observed in the rocks showed variation from horizontal to moderately dipping, which indicates that heterogeneous shear occurred in these rocks.

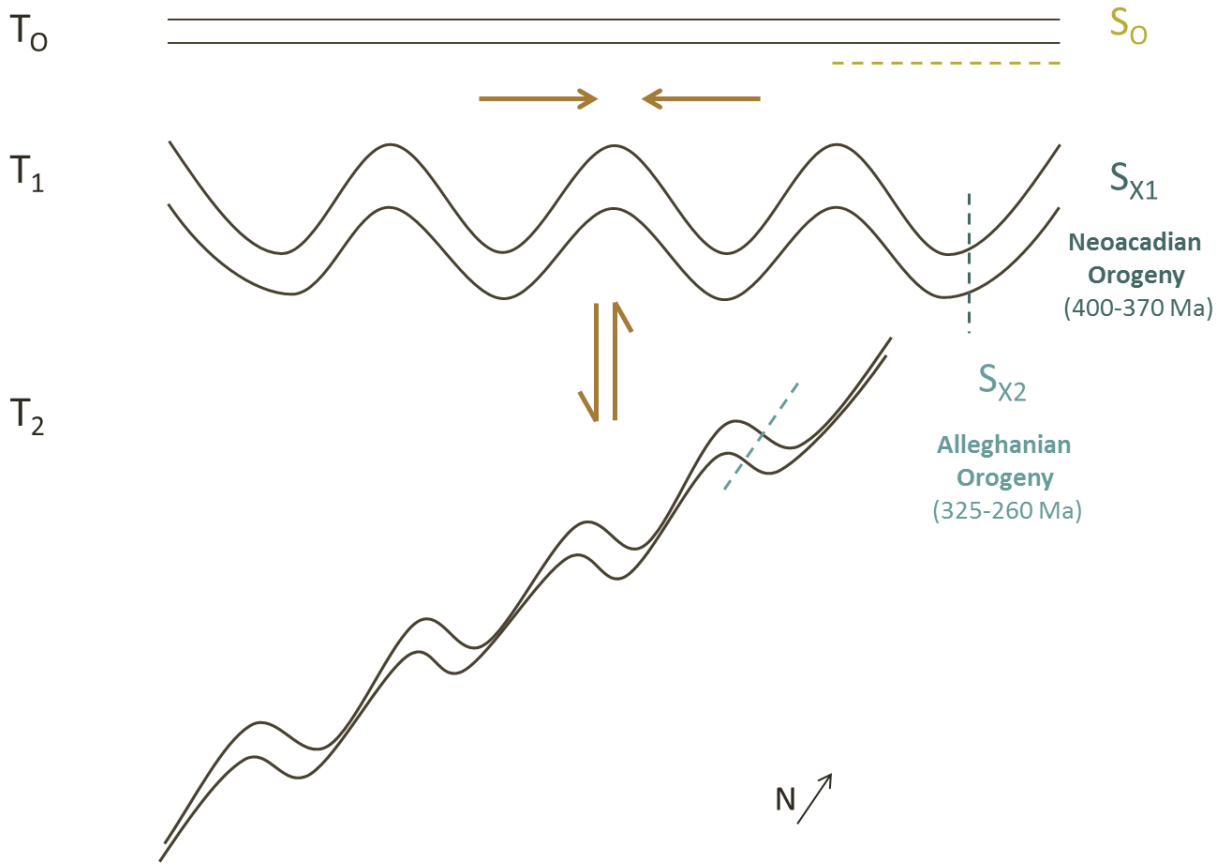

Figure 6.5: Diagram for the formation of the asymmetric folds observed in the Zone of Near Transposition in the HG slate. From T_0 to T_1 shortening occurred, forming buckle folds that are open and subrounded. From T_1 to T_2 shearing occurred (dextral), forming asymmetric folds.

Crenulation cleavage fabric occurs when an earlier planar fabric is overprinted by a later planar fabric, by recrystallization of mica minerals during metamorphism, when the second deformation is at an angle different to the original deformation. The intersection of the foliations causes a crenulation texture to develop. Crenulation foliation was not observed in the samples gathered at Cape St. Marys for this thesis, but there has been coaxial overprinting of

earlier formed fabrics (previously discussed above). Crenulation has been observed in other rocks from the White Rock Formation in samples collected from further east at Cape St. Marys (in Cape St. Marys Shear Zone) (Figure 6.6) (Culshaw & Liesa, 1997). Interpreted together at a regional scale, this leads to the hypothesis of White Rock Formation side-up plane strain simple shear (Figure 6.7 A&B). In the study area, at the northwest boundary of the Cape St. Marys Shear Zone, the direction of shear (WRF side-up) would transpose cleavage; the same direction of shear at the southeast boundary would form crenulations (as observed by Culshaw and Liesa, 1997).

Figure 6.6: S_2 crenulation fabric overprints continuous transposition cleavage (S_2 with S_0 parallel (sub-vertical in photo)) in Halifax Group slate, southeast boundary of Cape St. Marys Shear Zone (from Culshaw & Liesa, 1997).

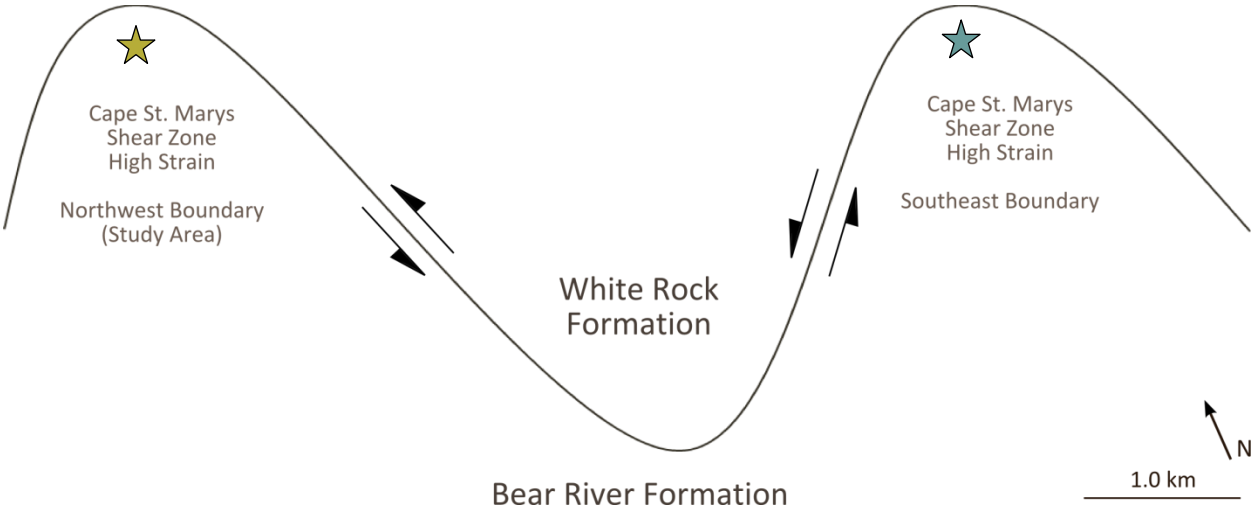

Figure 6.7A: Direction of shear across the unconformity between the Halifax Group and the White Rock Formation at the Cape St. Marys Shear Zone, explaining the observation of transposition and lack of crenulation at the study area, and the observation of crenulations at the southeast boundary.

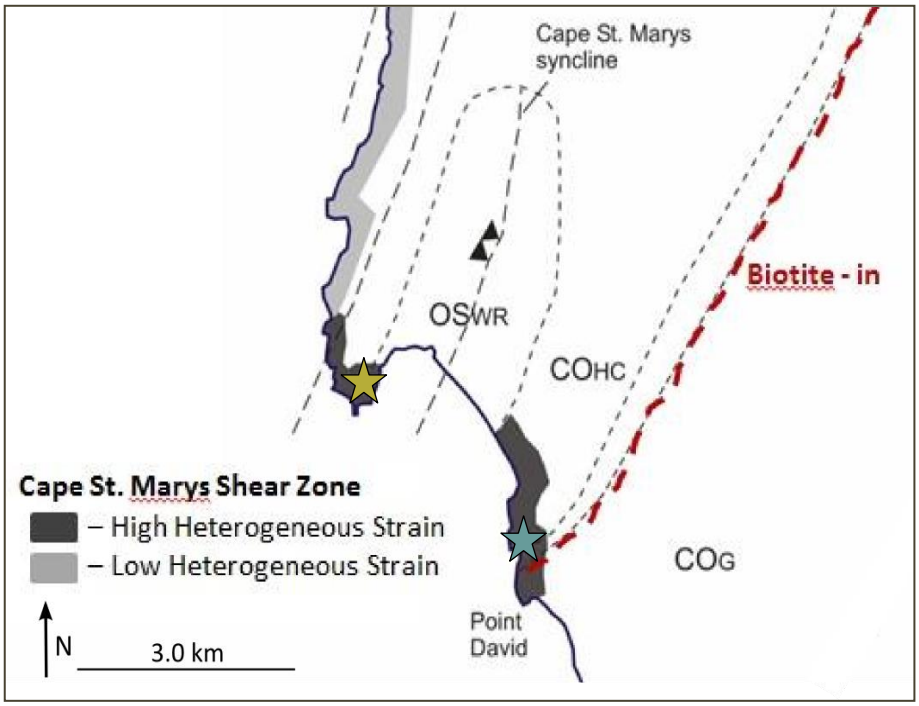

Figure 6.7B: Simplified geological outline of Cape St. Marys region showing the Cape St. Marys shear zone, axial traces of the Bear Cove synclinorium, and biotite-in isograd. Locations of Figure 6.4A observations indicated (modified from Culshaw & Liesa, 1997).

Chapter 7: Conclusions

Several important conclusions have been reached over the course of this thesis:

(1) the close angle between the S_0/S_{x1} fabric and the S_{x2} fabric in the Halifax Slate group imply the rocks have experienced a high strain;

(2) the variable intersection lineation in the HG slate from horizontal to moderately dipping suggests that the high strain was heterogeneous;

(3) there was extension in the down-dip direction of the S_{x2} plane, supported by the down-dip stretched lapilli (WRF dacite) and preserved *Arenicolites* burrows boudinaged down-dip (HG slate);

(4) evidence of shearing is supported by stretching lineation of quartz fringes on pyrites in the HG slate;

(5) no evidence of a discrete fault was found at or near to the contact, so deformation was continuous across the contact;

(6) the shape of the quartz-fringes, lack of crenulations and the asymmetric folds are consistent with plane strain simple shear of the region.

These deductions lead to the overall conclusion that the Halifax Group and the White Rock Formation deformed in-situ and did so by White Rock Formation side-up plane strain simple shear across the region, where the direction of shear has been interpreted from sheared folds.

7.1 Further Research

Further work is recommended to better understand the deformation at Cape St. Marys and southwestern Nova Scotia, the application of different techniques to refine the kinematics, and how microtectonic structure analysis can be utilized on other areas in the Northern Appalachians. Recommendations include:

- determining the age of recrystallization of quartz in the strain fringes, and whether the quartz crystals in the HG slate fringe structures and the WRF quartzite demonstrate a lattice preferred orientation (LPO) using complete electron back-scattered diffraction (EBSD);
- completing EBSD on the quartzite to also determine if the quartz has recorded Neoacadian phase deformation, Alleghanian phase deformation, or both; determine if the quartz veins in the quartzite can be correlated to either phase of deformation;
- test the use of fringe structures as kinematic indicators for progressive deformation in other units in southwest Nova Scotia to see if a consistent result is achieved.

References

Culshaw, N., & Lee, S. (2006). The Acadian fold belt in the Meguma Terrane, Nova Scotia: Cross sections, fold mechanisms, and tectonic implications. *Tectonics*. doi:10.1029/2004TC001752

Culshaw, N., & Liesa, M. (1997). Alleghanian reactivation of the Acadian fold belt, Meguma Zone, southwest Nova Scotia. *Canadian Journal of Earth Sciences*, 833-847.

Culshaw, N., & Reynolds, P. (1997). 40Ar/39Ar age of shear zones in the southwest Meguma Zone between Yarmouth and Metegran, Nova Scotia. *Canadian Journal of Earth Sciences*, 848-853.

Hicks, R., Jamieson, R., & Reynolds, P. (1999). Detrital and metamorphic 40Ar/39Ar ages from muscovite and whole-rock samples, Meguma Supergroup, southern Nova Scotia. *Canadian Journal of Earth Sciences, 36*(1), 23-32.

Hwang, S. (1985). Geology and structure of the Yarmouth area, southwestern Nova Scotia. *MSc Thesis, Acadia University*.

Keen, C., Kay, W., Keppie, D., Marillier, F., Pe-Piper, G., & Waldron, J. (1991). Deep seismic reflection data from the Bay of Fundy and Gulf of Maine: tectonic implications for the northern Appalachians. *Canadian Journal of Earth Sciences*, 1096-1111.

Keppie, D., Keppie, J., & Murphy, J. (2002). Saddle reef auriferous veins in a conical fold termination (Oldham anticlie, Meguma terrane, Nova Scotia, Canada): reconciliation of structural and age data. *Canadian Journal of Earth Sciences, 39*(1), 53-63.

Keppie, J., & Dallmeyer, R. (1987). Dating transcurrent terrane accretion: an example from the Meguma and Avalon composite terranes in the northern Appalachians. *Tectonics, 6*, 831-847.

Keppie, J., & Dallmeyer, R. (1987). Dating transcurrent terrane accretion: an example from the Meguma and Avalon composite terranes in the nothern Appalachians. *Tectonics*(6), 831-847.

Keppie, J., & Dallmeyer, R. (1995). Late Paleozoic collision, delamination, short-lived magmatism, and rapid denudation in the Meguma terrane (Nova Scotia, Canada): contraints from 40Ar/39Ar isotopic data. *Canadian Journal of Earth Sciences, 32*, 644-659.

Keppie, J., Fisher, B., & Poole, J. (2006). Geological Map of the Province of Nova Scotia. (2). Halifax, Nova Scotia, Canada. Retrieved August 2012, from http://www.gov.ns.ca/natr/meb/download/dp043.asp

Knaust, D., & Bromley, R. (2012). *Trace Fossils as Indicators of Sedimentary Environments.* Amsterdam: Elsevier.

Koehn, D., Bons, P., & Passchier, C. (2003). Development of antitaxial strain fringes during non-coaxial deforamtion: an experimental study. *Journal of Structural Geology*, 263-275.

MacDonald, L., Barr, S., White, C., & Ketchum, J. (2002). Petrology, age, and tectonic setting of the White Rock Formation, Meguma terrane, Nova Scotia: evidence for Silurian continental rifting. *Canadian Journal of Earth Sciences, 39*, 259-277.

Marshak, S. (2012). *Earth: Portrait of a Planet* (Vol. 4th Ed.). W.W. Norton Limited.

Muecke, G., Elias, P., & Reynolds, P. (1988). Hercynian/Alleghanian overprinting of an acadian terrane: 40Ar/39Ar studies in the Meguma zone, Nova Scotia, Canada. *Chemical Geology, 73*(2), 153-167.

Murphy, J., & Nance, R. (2008). The Pangea Conundrum. *Geology*, 703-706.

Passchier, C., & Trouw, R. (2005). *Microtectonics, 2 Ed.* Berlin: Springer-Verlag Berlin Heidelberg.

Raeside, R., & Jamieson, R. (1992). Low-pressure metamorphism of the Meguma Terrane, Nova Scotia. *Geological Association of Canada/Mineralogical Association of Canada Joint Annual Metting, Field Excursion C-5 Guidebook*.

Schenk, P. (1997). Sequence stratigraphy and provenance on Gondwana's margin: the Meguma Zone (Cambrian to Devonian) of Nova Scotia, Canada. *Geological Society of America Bulletin, 109*, 395-409.

Stipp, M., Stunitz, H., Heilbronner, R., & Schmid, S. (2002). The eastern Tonale fault zone: a 'natural laboratory' for crystal plastic deformation of quartz over a temperature range from 250 to 700 deg. C. *Journal of Structural Geology*, 1861-1884.

Twiss, R., & Moores, E. (2006). *Structural Geology, 2 Ed.* New York: W.H. Freeman and Company.

Waldron, J. (1992). The Goldenville-Halifax transition, Mahone Bay, Nova Scotia: relative sea-level change in the Meguma source terrane. *Canadian Journal of Earth Sciences, 29*, 1091-1105.

White, C. (2003). Prelimenary bedrock geology of the area between Chebogue Point, Yarmouth County, and Cape Sable Island, Shelburne County, southwestern Nova Scotia. *Mineral Resources Branch, Report of Activities 2002, Report 2003-1*, 127-145.

White, C. (2010). Stratigraphy of the Lower Paleozoic Goldenville and Halifax groups in southwestern Nova Scotia. *Atlantic Geology, 46*, 136-154.

White, C., & Barr, S. (2012). Meguma Terrane Revisited: Stratigraphy, Metamorphism, Paleontology, and Provenance. *Geoscience Canada, 39*(1). Retrieved December 2012, from http://journals.hil.unb.ca/index.php/gc/article/view/19450/21004

White, C., Horne, R., Teniere, P., Jodrey, M., & King, M. (2001). Geology of the Meteghan River-Yarmouth area: a progress report on the Southwest Nova Scotia Mapping Project. *Mineral and Energy Branch, Report of Activities 2000*, 95-111.

Williams, H. (1979). The Appalachian Orogen in Canada. *Canadian Journal of Earth Sciences*, 792-807.

Winter, J. (2010). *Principles of Igneous and Metamorphic Petrology.* Upper Saddle River, New Jersey: Pearson Prentice Hall.

Appendix I

Table 1: Summary of characteristics used for analysis of fringe structures in HG slate, and associated values in Table 2 (below Table 1).

Group	location of the pyrite core-object in relation to other core-objects in the groundmass	
	1 = core-object located in a group	
	0.5 = core-object located on the edge of a group	
	0 = core-object and associated fringe are isolated	
Shape	Elongated	Refers to shape of core-object (is one dimension longer than the other)
		1 = object is significantly longer in one dimension
		0.1 to 0.9 = one dimension of core-object is long than the other, but less significantly than 1
		0 = dimensions appear equal
	Equal	Refers to shape of core-object (are dimensions equal)
		1 = all dimensions appear equal
		0.1 to 0.9 = range where are approaching equal, but less significantly than 1
		0 = dimensions do not appear equal
Shear Direction	Dextral	Refers to the shear direction of strain fringe as dextral
		1 = indicators suggest shear direction was dextral
		0 = indicators do not suggest shear direction was dextral
	Sinistral	Refers to the shear direction of strain fringe as sinistral
		1 = indicators suggest shear direction was sinistral
		0 = indicators do not suggest shear direction was sinistral
	Unknown	Am I able to confidently determine the shear direction of strain fringe
		1 = shear direction cannot be determined from strain fringe
		0 = shear direction can be determine from strain fringe
Recrystallized	Grains in fringe structure show evidence of recrystallization	
	1 = yes, evidence of recrystallization is present throughout fringe	
	0.5 = partial recrystallization of fringe	
	0 = no evidence of recrystallization throughout fringe	
Growth of Fringe	Face-Controlled	Refers to growth direction of fringe crystals occurring in the opening direction
		1 = growth is face-controlled
		0.5 = growth is partially face-controlled
		0 = growth is not face-controlled
	Displacement-Controlled	Refers to growth direction of fringe crystals occurring normal to the object surface
		1 = growth is displacement=controlled
		0.5 = growth is partially displacement controlled
		0 = growth is not displacement controlled

Table 2: Complete table of analysis completed on HG Slate pyrite core-objects and their associated strain fringe (explanation to understand values provided in Table 1 on previous page).

Slide	Grain #	Shape	Group	Elongated	Equal	Dextral	Sinistral	Unknown	Recrystallized (Fringe)	Face - Controlled	Displacement - Controlled
cd_12_001a	1	subhedral	0	0.7	0.3	0	1	0	1	1	0
cd_12_001a	2	euhedral	1	0.8	0.2	0	1	0	1	1	0
cd_12_001a	3	euhedral	1	0.8	0.2	1	0	0	1	1	0
cd_12_001a	4	anhedral	1	0.8	0.2	0	0	1	1	0	0
cd_12_001a	5	subhedral	1	0.8	0.2	0	0	1	1	1	0
cd_12_001a	6	subhedral	1	0.2	0.8	0	1	0	1	0	1
cd_12_001a	7	anhedral	0	0.7	0.3	1	0	0	1	0	1
cd_12_001a	8	anhedral	0	0.2	0.8	0	0	1	1	0	0
cd_12_001a	9	subhedral	0	0.4	0.6	0	1	0	1	1	0
cd_12_001a	10	anhedral	1	0.4	0.6	0	0	1	1	1	0
cd_12_001a	11	euhedral	0	0.5	0.5	1	0	0	1	1	0
cd_12_001a	12	subhedral	0	1	0	0	1	0	1	0	1
cd_12_001a	13	euhedral	1	0.6	0.4	0	0	1	1	0	0
cd_12_001a	14	euhedral	1	0.2	0.8	0	0	1	1	0	0
cd_12_001a	15	subhedral	0	0.8	0.2	1	0	0	1	0	1
cd_12_001a	16	euhedral	1	0.7	0.3	0	0	1	1	1	0
cd_12_001a	17	euhedral	1	0.7	0.3	0	1	0	1	0	0
cd_12_001a	18	anhedral	1	0	1	0	1	0	1	1	0
cd_12_001a	19	subhedral	0	0.7	0.3	1	0	0	1	0	1
cd_12_001a	20	subhedral	0	0.8	0.2	1	0	0	1	1	0
cd_12_001a	21	euhedral	0	0	1	0	0	1	1	0	1
cd_12_001a	22	subhedral	0.5	0.9	0.1	1	0	0	1	0	1
cd_12_001a	23	subhedral	1	0.7	0.3	1	0	0	1	1	0
cd_12_001a	24	subhedral	1	1	0	0	1	0	1	1	0
cd_12_001a	25	anhedral	1	1	0	0	1	0	1	0	1
cd_12_001a	26	anhedral	1	0	1	0	1	0	1	0	1
cd_12_001a	27	anhedral	0.5	0	1	0	1	0	1	0	1
cd_12_001a	28	subhedral	0	0	1	0	0	1	1	1	0
cd_12_001a	29	anhedral	0.5	0.5	0.5	0	0	1	1	1	0
cd_12_001a	30	anhedral	1	0	1	0	0	1	1	1	0

Slide	Grain #	Shape	Group	Elongated	Equal	Dextral	Sinistral	Unknown	Recrystallized (Fringe)	Face - Controlled	Displacement - Controlled
cd_12_001a	31	anhedral	1	0.7	0.3	0	1	0	1	1	0
cd_12_001a	32	euhedral	0	1	0	0	1	0	1	1	0
cd_12_001a	33	subhedral	1	1	0	0	0	1	1	0	0
cd_12_001a	34	subhedral	1	0	1	0	0	1	1	1	0
cd_12_001a	35	subhedral	1	0.6	0.4	0	0	1	1	1	0
cd_12_001a	36	subhedral	1	1	0	0	0	1	1	0	0
cd_12_001a	37	subhedral	1	1	0	0	0	1	1	1	0
cd_12_001a	38	anhedral	1	1	0	1	0	0	1	0	0
cd_12_001a	39	euhedral	0	0.7	0.3	0	1	0	1	0	1
cd_12_001a	40	euhedral	0.5	0.8	0.2	0	1	0	1	0	1
cd_12_001a	41	euhedral	1	1	0	0	1	0	1	1	0
cd_12_001a	42	euhedral	0	0.8	0.2	0	1	0	1	0	1
cd_12_001a	43	euhedral	0.5	0.2	0.8	1	0	0	1	0	1
cd_12_001a	44	euhedral	1	0	1	0	0	1	1	0	0
cd_12_001a	45	euhedral	1	0	1	0	0	1	1	0	0
cd_12_001a	46	euhedral	1	1	0	0	1	0	1	0	1
cd_12_001a	47	euhedral	1	1	0	0	1	0	1	0	1
cd_12_001a	48	anhedral	1	0.7	0.3	0	1	0	1	0	0
cd_12_001a	49	anhedral	1	0.7	0.3	0	0	1	1	0	1
cd_12_001a	50	subhedral	0.5	1	0	0	0	1	1	0	1
cd_12_001a	51	subhedral	0.5	0.6	0.4	0	1	0	1	0	1
cd_12_001a	52	anhedral	0	0.6	0.4	0	1	0	1	0	1
cd_12_001a	53	euhedral	0	0.6	0.4	0	0	1	1	0	0
cd_12_001a	54	euhedral	0	0.6	0.4	1	0	0	1	0	0
cd_12_001a	55	euhedral	1	1	0	0	1	0	1	1	0
cd_12_001a	56	euhedral	1	0	1	0	0	1	1	0	0
cd_12_001a	57	subhedral	1	0.7	0.3	0	0	1	1	0	0
cd_12_001a	58	euhedral	0	0	1	0	0	1	1	1	0
cd_12_001a	59	subhedral	1	0.6	0.4	0	0	1	1	1	0
cd_12_001a	60	euhedral	1	0.6	0.4	0	1	0	1	0	1
cd_12_001a	61	subhedral	1	0	1	0	1	0	1	0	1
cd_12_001a	62	subhedral	0	0.7	0.3	0	0	1	1	0	0

Slide	Grain #	Shape	Group	Elongated	Equal	Dextral	Sinistral	Unknown	Recrystallized (Fringe)	Face - Controlled	Displacement - Controlled
cd_12_001a	63	anhedral	0	0.7	0.3	1	0	0	1	0	1
cd_12_001a	64	subhedral	0	0.7	0.3	1	0	0	1	1	0
cd_12_001a	65	euhedral	1	0	1	0	0	1	1	1	0
cd_12_001a	66	anhedral	0	0.7	0.3	0	1	0	1	0	1
cd_12_001a	67	anhedral	0	0.6	0.4	1	0	0	1	0	1
cd_12_001a	68	subhedral	0.5	0.7	0.3	0	1	0	1	0	1
cd_12_001a	69	euhedral	1	0.8	0.2	0	0	1	1	1	0
cd_12_001a	70	subhedral	1	0.8	0.2	1	0	0	1	1	0
cd_12_001a	71	euhedral	1	0.2	0.8	0	0	1	1	1	0
cd_12_001a	72	anhedral	1	0.8	0.2	0	1	0	1	1	0
cd_12_001a	73	subhedral	1	0.8	0.2	0	0	1	1	0	1
cd_12_001a	74	euhedral	1	0	1	1	0	0	1	0	1
cd_12_001a	75	euhedral	1	1	0	1	0	0	1	0	1
cd_12_001a	76	anhedral	1	0	1	1	0	0	1	1	0
cd_12_001b	77	euhedral	0	0.2	0.8	0	0	1	1	1	0
cd_12_001b	78	subhedral	0.5	0	1	0	0	1	1	1	0
cd_12_001b	79	euhedral	0.5	0	1	0	0	1	1	1	0
cd_12_001b	80	subhedral	1	0	1	0	0	1	1	1	0
cd_12_001b	81	euhedral	1	0	1	0	1	0	1	0.5	0.5
cd_12_001b	82	euhedral	1	0	1	0	0	1	1	1	0
cd_12_001b	83	anhedral	1	0.5	0.5	0	0	1	1	0.5	0.5
cd_12_001b	84	subhedral	1	0	1	0	1	0	1	0	1
cd_12_001b	85	subhedral	1	0	1	1	0	0	1	0.5	0.5
cd_12_001b	86	anhedral	1	0.5	0.5	1	0	0	1	0.5	0.5
cd_12_001b	87	anhedral	1	0.8	0.2	0	1	0	1	0	1
cd_12_001b	88	subhedral	1	0.7	0.3	0	1	0	1	0.5	0.5
cd_12_001b	89	subhedral	0.5	1	0	0	1	0	1	0	1
cd_12_001b	90	anhedral	1	0.5	0.5	0	0	1	1	0	1
cd_12_001b	91	anhedral	1	0.5	0.5	0	0	1	1	0.5	0.5
cd_12_001b	92	subhedral	1	0	1	0	1	0	1	0	1
cd_12_001b	93	subhedral	1	0.8	0.2	0	1	0	1	0.5	0.5
cd_12_001b	94	anhedral	1	0.7	0.3	0	0	1	1	0	1

Slide	Grain #	Shape	Group	Elongated	Equal	Dextral	Sinistral	Unknown	Recrystallized (Fringe)	Face - Controlled	Displacement - Controlled
cd_12_001b	95	euhedral	1	0	1	0	1	0	1	0.5	0.5
cd_12_001b	96	subhedral	0.5	0.8	0.2	0	1	0	1	0	1
cd_12_001b	97	euhedral	0.5	0.8	0.2	0	1	0	1	0	1
cd_12_001b	98	anhedral	0.5	1	0	0	1	0	1	0.5	0.5
cd_12_001b	99	subhedral	0.5	0.6	0.4	0	0	1	0	0	1
cd_12_001b	100	anhedral	0	0	1	1	0	0	1	0	1
cd_12_001b	101	anhedral	1	0.6	0.4	1	0	0	1	1	0
cd_12_001b	102	euhedral	0.5	1	1	0	1	0	0.5	0.5	0.5
cd_12_001b	103	euhedral	1	0.8	0.2	0	1	0	1	0.5	0.5
cd_12_001b	104	euhedral	1	0	1	0	0	1	0.5	1	0
cd_12_001b	105	euhedral	0.5	0.7	0.3	1	0	0	1	0.5	0.5
cd_12_001b	106	subhedral	0.5	0.7	0.3	0	0	1	1	0	1
cd_12_001b	107	subhedral	0.5	0.7	0.3	0	0	1	1	0.5	0.5
cd_12_001b	108	euhedral	0.5	0.6	0.4	0	1	0	1	0	1
cd_12_001b	109	euhedral	0.5	0	1	0	0	1	1	1	0
cd_12_001b	110	subhedral	0.5	0.6	0.4	0	0	1	1	0	1
cd_12_001b	111	subhedral	0.5	0.5	0.5	0	1	0	0.5	1	0
cd_12_001b	112	euhedral	1	0	1	0	1	0	1	0.5	0.5
cd_12_001b	113	subhedral	0	0	1	0	1	0	1	0.5	0.5
cd_12_001b	114	anhedral	0	0.7	0.3	0	0	1	1	0	1
cd_12_001b	115	subhedral	1	0.8	0.2	0	0	1	1	0	1
cd_12_001b	116	subhedral	1	0.5	0.5	0	0	1	1	0	1
cd_12_001b	117	anhedral	1	0.7	0.3	0	0	1	1	0.5	0.5
cd_12_001b	118	euhedral	1	1	0	0	0	1	1	0.5	0.5
cd_12_001b	119	subhedral	1	1	0	0	1	0	1	0	1
cd_12_001b	120	euhedral	0.5	0	1	1	0	0	1	0	1
cd_12_001b	121	euhedral	1	0.7	0.3	0	1	0	0.5	0	1
cd_12_001b	122	subhedral	1	0.7	0.3	0	0	1	0.5	0	1
cd_12_001b	123	subhedral	1	0.6	0.4	0	0	1	0.5	0	1
cd_12_001b	124	subhedral	1	0.5	0.5	0	1	0	1	0	1
cd_12_001b	125	anhedral	1	0.2	0.8	1	0	0	1	0	1
cd_12_001b	126	anhedral	1	0	1	0	1	0	1	0.5	0.5

Slide	Grain #	Shape	Group	Elongated	Equal	Dextral	Sinistral	Unknown	Recrystallized (Fringe)	Face - Controlled	Displacement - Controlled
cd_12_001b	127	subhedral	1	0	1	0	1	0	1	0.5	0.5
cd_12_001b	128	subhedral	1	0.5	0.5	1	0	0	1	0.5	0.5
cd_12_001b	129	subhedral	1	0	1	0	0	1	1	0.5	0.5
cd_12_001b	130	subhedral	1	0.5	0.5	0	0	1	1	0.5	0.5
cd_12_001b	131	subhedral	1	0	1	0	0	1	1	0.5	0.5
cd_12_004a	132	euhedral	0.5	0.6	0.4	0	1	0	1	0.5	0.5
cd_12_004a	133	euhedral	0.5	0.6	0.4	0	0	1	1	0	1
cd_12_004a	134	subhedral	0	0.7	0.3	0	0	1	1	0.5	0.5
cd_12_004a	135	anhedral	1	1	0	1	0	0	1	0.5	0.5
cd_12_004a	136	euhedral	1	0	1	0	1	0	1	0.5	0.5
cd_12_004a	137	anhedral	1	0.6	0.4	0	0	1	1	0.5	0.5
cd_12_004a	138	subhedral	0	0	1	1	0	0	1	0.5	0.5
cd_12_004a	139	anhedral	1	0.6	0.4	0	1	0	1	0	1
cd_12_004a	140	euhedral	1	1	0	0	0	1	1	0.5	0.5
cd_12_004a	141	euhedral	1	1	0	1	0	0	1	0.5	0.5
cd_12_004a	142	subhedral	1	1	0	0	0	1	1	0.5	0.5
cd_12_004a	143	anhedral	1	0.6	0.4	0	1	0	1	0.5	0.5
cd_12_004a	144	euhedral	1	1	0	0	0	1	1	0	1
cd_12_004a	145	euhedral	1	1	0	0	1	0	1	0	1
cd_12_004a	146	subhedral	1	0	1	1	0	0	1	0.5	0.5
cd_12_004a	147	euhedral	1	1	0	0	0	1	0	0.5	0.5
cd_12_004a	148	euhedral	1	1	0	1	0	0	1	0.5	0.5
cd_12_004a	149	subhedral	0.5	1	0	1	0	0	1	0.5	0.5
cd_12_004a	150	anhedral	0.5	0.6	0.4	0	0	1	0	0	1
cd_12_004a	151	subhedral	0	1	0	0	1	0	0	0.5	0.5
cd_12_004a	152	subhedral	0	1	0	0	1	0	1	0.5	0.5
cd_12_004a	153	subhedral	0	0.7	0.3	1	0	0	1	0	1
cd_12_004a	154	anhedral	1	0.6	0.4	0	1	0	1	0	1
cd_12_004a	155	subhedral	1	0.6	0.4	0	1	0	1	0	1
cd_12_004a	156	anhedral	1	0.6	0.4	0	0	1	1	0	1
cd_12_004a	157	subhedral	1	0.6	0.4	0	1	0	1	0	1
cd_12_004a	158	subhedral	1	0.6	0.4	1	0	0	1	0	1

Slide	Grain #	Shape	Group	Elongated	Equal	Dextral	Sinistral	Unknown	Recrystallized (Fringe)	Face - Controlled	Displacement - Controlled
cd_12_004a	159	anhedral	1	1	0	0	0	1	1	1	1
cd_12_004a	160	anhedral	0	1	0	1	0	0	1	0	1
cd_12_004a	161	subhedral	0	1	0	0	1	0	1	0	1
cd_12_004a	162	anhedral	1	0.6	0.4	0	1	0	1	0.5	0.5
cd_12_004a	163	subhedral	1	1	0	0	1	0	1	0	1
cd_12_004a	164	anhedral	1	0.7	0.3	1	0	0	1	0	1
cd_12_004a	165	subhedral	1	0.7	0.3	0	1	0	1	0.5	0.5
cd_12_004a	166	anhedral	1	0.6	0.4	0	1	0	1	0.5	0.5
cd_12_004a	167	anhedral	0.5	0.6	0.4	0	1	0	1	0	1
cd_12_004a	168	subhedral	1	0	1	0	0	1	1	0	1
cd_12_004b	169	euhedral	0.5	0.8	0.2	0	1	0	1	0	1
cd_12_004b	170	euhedral	1	0.8	0.2	0	1	0	1	0	1
cd_12_004b	171	subhedral	1	0	1	0	0	1	1	0.5	0.5
cd_12_004b	172	anhedral	1	1	0	1	0	0	1	0	1
cd_12_004b	173	subhedral	1	0.6	0.4	0	1	0	1	0	1
cd_12_004b	174	subhedral	1	0.6	0.4	0	0	1	1	0	1
cd_12_004b	175	euhedral	0	1	0	0	1	0	0	0	1
cd_12_004b	176	subhedral	1	0.8	0.2	0	1	0	1	0.5	0.5
cd_12_004b	177	euhedral	0	1	0	0	1	0	1	0.5	0.5
cd_12_004b	178	euhedral	0	1	0	1	0	0	1	0	1
cd_12_004b	179	euhedral	0.5	1	0	0	1	0	1	0	1
cd_12_004b	180	euhedral	0.5	1	0	0	0	1	1	0	1
cd_12_004b	181	anhedral	1	0	1	0	1	0	1	0.5	0.5
cd_12_004b	182	anhedral	0.5	0	1	0	1	0	1	0	1
cd_12_004b	183	anhedral	1	0.5	0.5	0	1	0	1	0.5	0.5
cd_12_004b	184	subhedral	1	1	0	0	0	1	1	0	1
cd_12_004b	185	subhedral	0	1	0	1	0	0	1	0.5	0.5
cd_12_004b	186	subhedral	0.5	1	0	0	0	1	1	0	1
cd_12_004b	187	anhedral	0.5	0	1	0	1	0	1	0	1
cd_12_004b	188	subhedral	1	0.5	0.5	0	1	0	1	0.5	0.5
cd_12_004b	189	euhedral	0	0	1	0	1	0	1	0.5	0.5
cd_12_004b	190	subhedral	0	0	1	0	0	1	1	0	1

Slide	Grain #	Shape	Group	Elongated	Equal	Dextral	Sinistral	Unknown	Recrystallized (Fringe)	Face - Controlled	Displacement - Controlled
cd_12_004b	191	anhedral	0	0	1	0	0	1	1	0	1
cd_12_004b	192	anhedral	0	0.6	0.4	0	0	1	1	0.5	0.5
cd_12_004b	193	anhedral	0	1	0	0	0	1	1	0	1
cd_12_004b	194	anhedral	0	0	1	0	0	1	1	0.5	0.5
cd_12_004b	195	euhedral	0.5	1	0	0	0	1	1	0.5	0.5
cd_12_004b	196	subhedral	1	1	0	0	1	0	1	0.5	0.5
cd_12_004b	197	subhedral	1	0.7	0.3	0	0	1	1	0	1
cd_12_004b	198	euhedral	1	0.6	0.4	0	0	1	1	0.5	0.5
cd_12_004b	199	subhedral	0	1	0	0	0	1	1	0.5	0.5
cd_12_004b	200	subhedral	0	1	0	0	0	1	1	0	1
cd_12_004b	201	anhedral	0	1	0	0	0	1	1	0.5	0.5
cd_12_004b	202	euhedral	0	0	1	1	0	0	1	0	1
cd_12_004b	203	euhedral	0	0	1	0	1	0	1	0.5	0.5
cd_12_004b	204	euhedral	0	0	1	0	0	1	1	0.5	0.5
cd_12_004b	205	anhedral	0.5	0	1	0	1	0	1	0	1
cd_12_004b	206	subhedral	0.5	0	1	0	1	0	1	0	1
cd_12_004b	207	subhedral	0.5	0	1	0	1	0	1	0.5	0.5
cd_12_004b	208	euhedral	0.5	0	1	0	0	1	1	0	1
cd_12_004b	209	euhedral	0.5	0	1	0	0	1	1	0	1
cd_12_004b	210	subhedral	0.5	0	1	0	0	1	1	0	1
cd_12_004b	211	subhedral	1	0	1	0	1	0	1	0.5	0.5
cd_12_004b	212	subhedral	0.5	0	1	0	1	0	1	0.5	0.5
cd_12_004b	213	euhedral	1	0	1	0	1	0	1	0.5	0.5
cd_12_004b	214	euhedral	1	0	1	0	1	0	1	0.5	0.5
cd_12_004b	215	subhedral	0	0	1	0	1	0	1	0.5	0.5
cd_12_004b	216	anhedral	0	0	1	0	0	1	1	0	1
cd_12_004b	217	anhedral	0	0	1	0	1	0	1	0	1
cd_12_004b	218	euhedral	0	0	1	0	1	0	1	0.5	0.5
cd_12_004b	219	subhedral	1	0	1	0	1	0	1	0.5	0.5

Appendix II

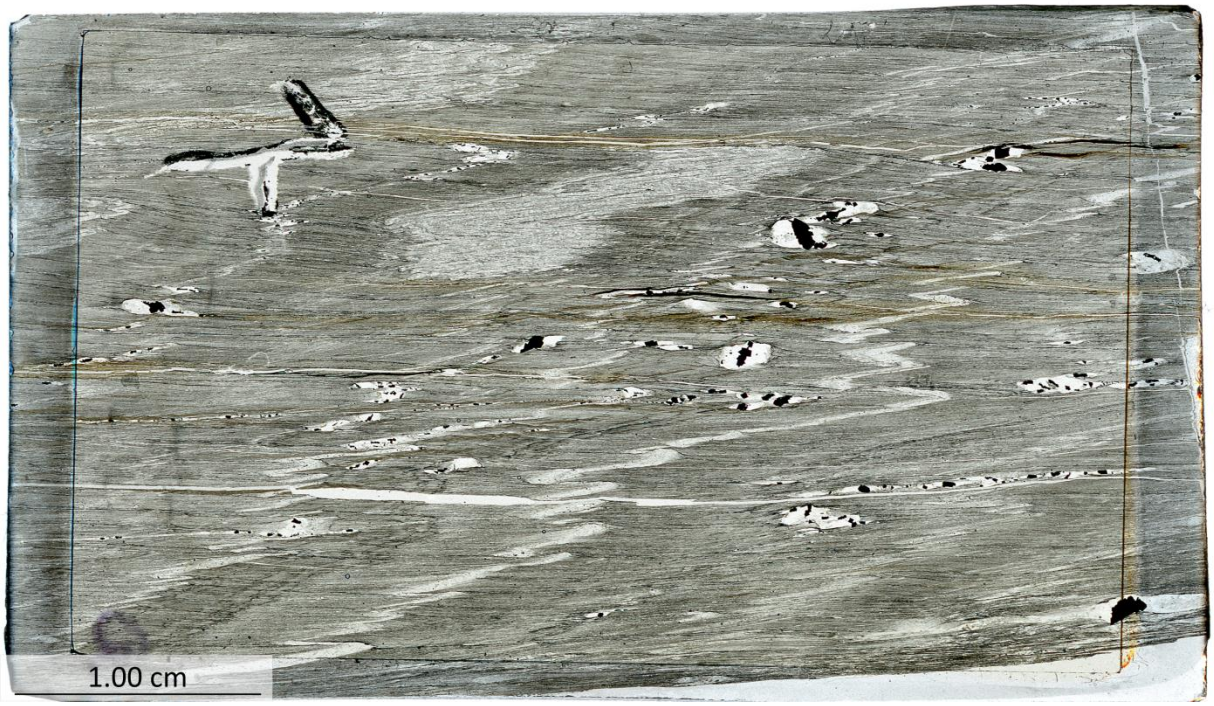

Sample CD_12_001a (HG slate) – Station 014

Sample CD-12_001b (HG slate) – Station 014

Sample CD_12_002 (WRF dacite) – Station 009

Sample CD_12_003a (WRF dacite) – Station 009

Sample CD_12_003b (WRF dacite) – Station 009

Sample CD_12_003c (WRF dacite) – Station 009

Sample CD_12_004a (HG slate) – Station 008

Sample CD_12_004b (HG slate) – Station 008

Sample CD_12_004c (HG slate) – Station 008

Sample CD_12_008a (WRF dacite) – Station 009

Sample CD_12_008b (WRF dacite) – Station 009

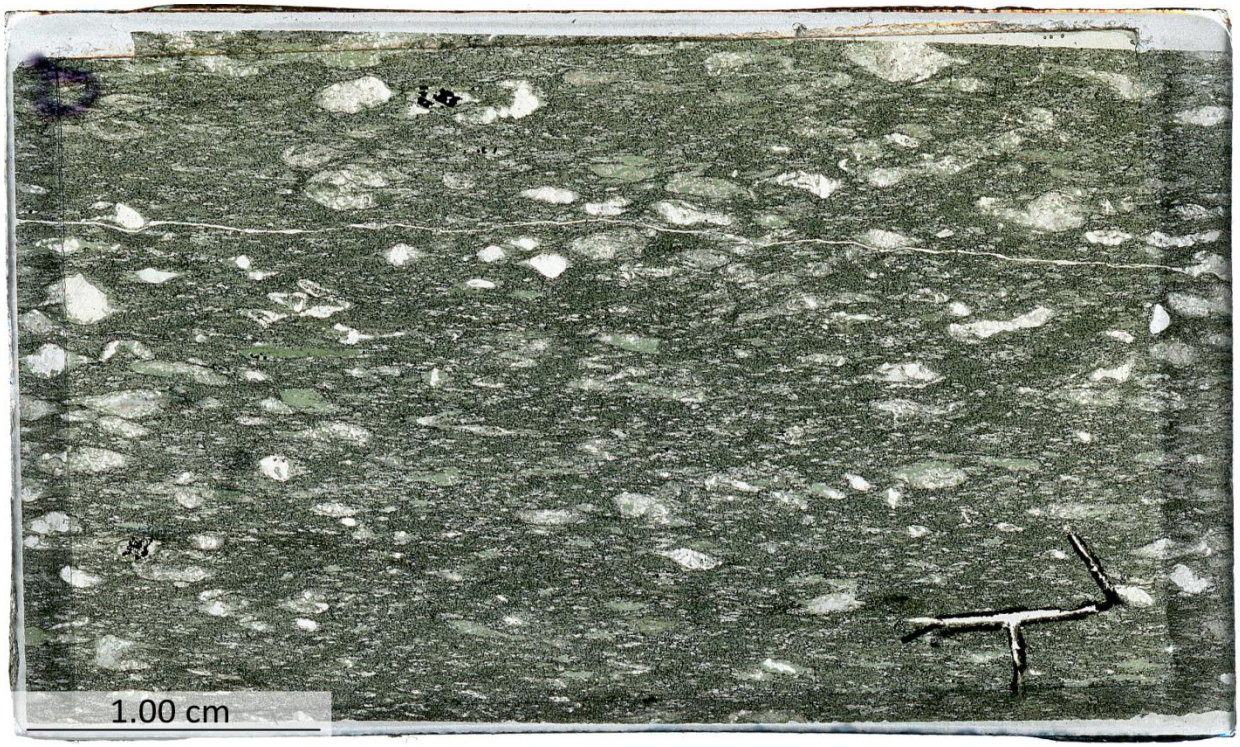

Sample CD_12_009a (WRF Greenschist Basalt) – Station 010

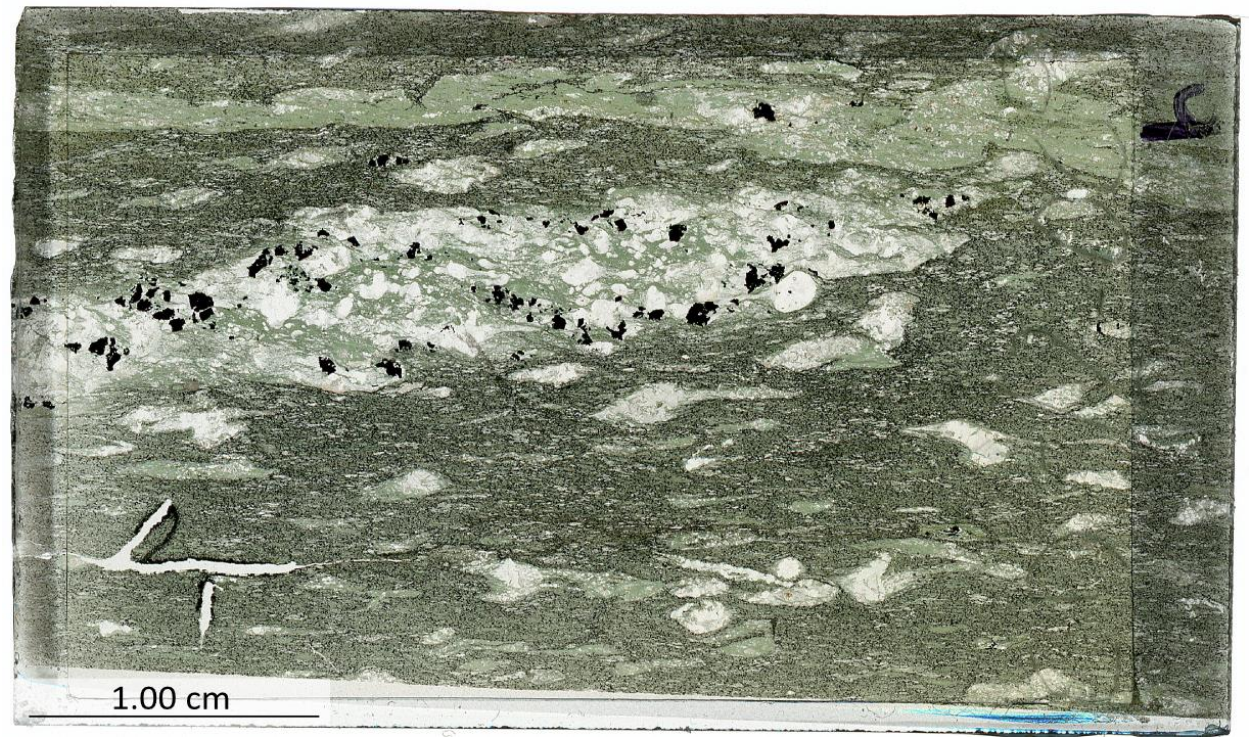

Sample CD_12_009b (WRF Greenschist Basalt) – Station 010

Sample CD_12_009c (WRF Greenschist Basalt) – Station 010

Sample JF_05_1010 (WRF quartzite) – Station 013